Supplementary Information for

# *J*-driven Dynamic Nuclear Polarization for sensitizing high field solution state NMR

*Maria Grazia Concilio[1*], Ilya Kuprov[2], Lucio Frydman,[1,3*]*

[1]Department of Chemical and Biological Physics, Weizmann Institute of Science, Rehovot, Israel.

[2]School of Chemistry, University of Southampton, Southampton, UK.

[3]National High Magnetic Field Laboratory, Tallahassee, Florida, USA.

**Supporting Information 1: $R_1/R_2$ relaxation rate analysis for mono- and bis-trityl radicals**

As this is a purely theoretical study, we consider it necessary to test our numerical simulations against experimental measurements. Given the paucity of solution-state NMR data about relaxation rates in biradicals, theoretical models were used to estimate electron longitudinal and transverse relaxation rates for trityl monoradicals – for which solution-state measurements have been reported in [1,2]. Following the treatment in [1], electron $R_1$ rate for this radical will be assumed to have three contributions:

$$R_{1,\text{total}} = R_{1,\text{local}} + R_{1,\text{BRW}} + R_{1,\text{solvent}}$$

$$\approx R_{1,\text{local}} + R_{1,\text{BRW}} \tag{S1a}$$

Here $R_{1,\text{local}}$ is the self-relaxation rate arising from the local vibrational modes related to the stretching of bonds in the radical, and is a magnetic field independent contribution estimated by Eaton et al [1] as $5.9 \times 10^4$ Hz for per-deutero and $6.1 \times 10^4$ Hz for per-protio trityls. The Redfield component:

$$R_{1,\text{BRW}} = n \underbrace{\left[ \left( \frac{\Delta^2_{\text{HF,intra}}}{9} \right) \left( \frac{\tau_C}{\left(1 + \tau_C^2 \omega_E^2\right)} \right) \right]}_{\text{hyperfine relaxation}} + \underbrace{\left( \frac{2\Delta^2_G}{15} \right) \left( \frac{\tau_C}{\left(1 + \tau_C^2 \omega_E^2\right)} \right)}_{\text{g-anisotropy relaxation}} \tag{S1b}$$

is the relaxation rate which arises from the stochastic modulation of the radical's *g*-tensor anisotropy and of the hyperfine interactions between the electron and the n protons interacting with it within the radical (that in the case of a trityl monomer can be considered approximately the same); this is the kind of rate computed in the main text based on Bloch-Redfield-Wangsness theory in terms of $\Delta^2_G$ and $\Delta^2_{\text{HF,intra}}$ coupling strengths; i.e., of the second-rank norm Blicharsky squared,[3] already mentioned in the main text and defined in Eq. S58 in Supporting Information 5, for the *g*-anisotropy and the hyperfine interaction tensors. Finally,

$$R_{1,\text{solvent}} = n_{\text{solv}} \left[ \left( \frac{\Delta^2_{\text{HF,inter}}}{9} \right) \frac{\tau_{\text{solv}}}{\left(1 + \tau_{\text{solv}}^2 \omega_E^2\right)} \right] \tag{S1c}$$

is an *ad hoc* relaxation term, arising from the dipolar interaction between the electron and $n_{\text{solv}}$ solvent molecules; the coupling strength of this relaxation is given by the second-rank norm squared of the dipolar interaction tensor between the electron and the solvent protons $\Delta^2_{\text{HF,inter}}$, and by a correlation time $\tau_{\text{solvent}}$. Eaton et al in [1] have estimated the $R_{1,\text{solvent}}$ in Eq. (S1c) as $\tau_{\text{solv}} = F \tau_C$, where F is a

ratio between the solvent correlation time and the trityl correlation time, that is different for each radical. As this latter term is much smaller than the remaining relaxation rates it is henceforth ignored in both the mono- and bi-radical estimations. Finally, in a non-viscous solvent, the $R_{2,total}$ corresponds to $R_{1,total} + R_{2,BRW}$ [1]. The BRW theory predicts this second term to be:

$$R_{2,\text{BRW}} = n\left[\underbrace{\left(\frac{\Delta_{\text{HF,trityl}}^2}{90}\right)\left(2+\frac{5\tau_{\text{C}}}{\left(1+\tau_{\text{C}}^2\omega_{\text{E}}^2\right)}+\frac{3\tau_{\text{C}}}{\left(1+\tau_{\text{C}}^2\omega_{\text{N}}^2\right)}\right)}_{\text{hyperfine relaxation}}\right]+\underbrace{\left(\frac{\Delta_{\text{G}}^2}{45}\right)\left(4+\frac{3\tau_{\text{C}}}{\left(1+\tau_{\text{C}}^2\omega_{\text{E}}^2\right)}\right)}_{\text{g-anisotropy relaxation}}$$  (S2)

Table S1 compares the $R_{1,total}$ and $R_{2,total}$ values determined from Eqs. (S1a) and (S2), with values reported experimentally in [1] for per-protio and per-deutero trityls at different fields. There is good agreement between both sets. Notice, however, that the low magnetic fields explored in this comparison, it is the local vibrational modes contributing to $R_{1,local}$ that dominate the longitudinal- and transverse relaxation rates. As this parameter was estimated from the experimental data, the good agreement is not surprising.

**Table S1:** Comparison between $T_1$ and $T_2$ calculated using Eq. (S1a) and Eq. (S2) and experimental $T_1$ and $T_2$ in water for trityl-$CD_3$ and trityl-$CH_3$ obtained from [1]. n represents the number of trityl protons dipole-coupled to the radical. For trityl-$CH_3$, the distances between the electron and all 36 protons in the radical were set equal to 5.3 Å.

| Magnetic field / T | $R_1$ from Eq. 1 / Hz | Experimental $R_1$ / Hz | $R_2$ from Eq. 2 / Hz | Experimental $R_2$ / Hz |
|---|---|---|---|---|
| Trityl-$CD_3$ radical, n = 0, $R_{1,local}$= 0.59 x $10^5$ Hz | | | | |
| 0.33 T (X-band) | 5.9x$10^4$ | 5.9x$10^4$ | 6.7x$10^4$ | 9.1x$10^4$ |
| 0.11 T (S-band) | 5.9x$10^4$ | 6.2x$10^4$ | 6.2x$10^4$ | 8.3x$10^4$ |
| 0.03 T (L-band) | 5.9x$10^4$ | 7.2x$10^4$ | 6.2x$10^4$ | 8.3x$10^4$ |
| 9 x$10^{-3}$ T (250 MHz) | 6.2x$10^4$ | / | 6.2x$10^4$ | 9.1x$10^4$ |
| Trityl-$CH_3$ radical → n = 36, $R_{1,local}$ = 0.61 x $10^5$ Hz | | | | |
| 0.33 T (X-band) | 6.2x$10^4$ | 6.2x$10^4$ | 2.3x$10^5$ | 1.1x$10^5$ |
| 0.11 T (S-band) | 6.6x$10^4$ | 7.1x$10^4$ | 1.0x$10^5$ | 1.1x$10^5$ |
| 0.03 T (L-band) | 8.3x$10^4$ | 8.3x$10^4$ | 1.1x$10^5$ | 1.1x$10^5$ |
| 9 x$10^{-3}$ T (250 MHz) | 9.1x$10^4$ | / | 1.3x$10^5$ | 1.3x$10^5$ |

It is enlightening to extend this monoradical analysis to the case of trityl bi-radicals. In this case it is reasonable to assume that the contributions coming from solvent-induced and bond-vibration-induced terms to $R_1$ relaxation, will remain similar as those given in Table S1. The electron $R_{1,BRW}$ and $R_{2,BRW}$ longitudinal and transverse rates, however, will be significantly increased by the electron-electron dipolar interaction, and will now be dominated by $J(0)$-containing terms that depend on the rotational correlation time but are independent of the magnetic field. A full analysis of these two terms using symbolic processing software[4] leads to:

$$R_{1,\text{BRW}} = -R\left[\hat{E}_Z\right] = \frac{\Delta_{\text{EE}}^2}{90} J(0) + \frac{\aleph_{(\text{HFC},\Sigma\text{HF}),\text{inter}}}{18} J(\omega_E) +$$

$$+\frac{\aleph_{(\text{HFC},\Delta\text{HF}),\text{inter}}}{360} \left[\begin{array}{l} 3J(J_{\text{ex}} + \omega_E) + 3J(J_{\text{ex}} - \omega_E) + 6J(J_{\text{ex}} + \omega_E + \omega_N) + \\ +6J(J_{\text{ex}} - \omega_E - \omega_N) + J(J_{\text{ex}} + \omega_E - \omega_N) + J(J_{\text{ex}} - \omega_E + \omega_N) \end{array}\right] +$$

$$+n\left(\begin{array}{l} \dfrac{\aleph_{(\text{HFC},\Sigma\text{HF}),\text{intra}}}{18} J(\omega_E) + \\[2mm] \dfrac{\aleph_{(\text{HFC},\Delta\text{HF}),\text{intra}}}{360} \left[\begin{array}{l} 3J(J_{\text{ex}} + \omega_E) + 3J(J_{\text{ex}} - \omega_E) + 6J(J_{\text{ex}} + \omega_E + \omega_N) + \\ +6J(J_{\text{ex}} - \omega_E - \omega_N) + J(J_{\text{ex}} + \omega_E - \omega_N) + J(J_{\text{ex}} - \omega_E + \omega_N) \end{array}\right] \end{array}\right) +$$

$$+\frac{\left[4\aleph_{G,\Delta G} + 2\aleph_{\text{EE},-\Delta G}\right]}{120} J(J_{\text{ex}} - \omega_E) + \frac{\left[4\aleph_{G,\Delta G} + 2\aleph_{\text{EE},\Delta G}\right]}{120} J(J_{\text{ex}} + \omega_E) +$$

$$+\frac{\left[3\Delta_{\text{EE}}^2 + 6\aleph_{G,\Sigma G}\right]}{90} J(\omega_E) + \frac{\Delta_{\text{EE}}^2}{15} J(2\omega_E) \tag{S3}$$

and

$$R_{2,\text{BRW}} = -R\left[\hat{E}_+\right] = \frac{\Delta_{\text{EE}}^2}{36} J(0) + \frac{4\aleph_{G,\Sigma G}}{90} J(0) +$$

$$+\frac{\aleph_{(\text{HFC},\Sigma\text{HF}),\text{inter}}}{90} J(0) + \frac{\aleph_{(\text{HFC},\Sigma\text{HF}),\text{inter}}}{120} J(\omega_N) + \frac{\aleph_{(\text{HFC},\Sigma\text{HF}),\text{inter}}}{36} J(\omega_E) +$$

$$+\frac{\aleph_{(\text{HFC},\Delta\text{HF}),\text{inter}}}{720} \left[\begin{array}{l} 3J(J_{\text{ex}} - \omega_E) + 3J(J_{\text{ex}} + \omega_E) + 12J(J_{\text{ex}} - \omega_E - \omega_N) + 12J(J_{\text{ex}} + \omega_E - \omega_N) + \\ +J(J_{\text{ex}} - \omega_E + \omega_N) + 6J(J_{\text{ex}} + \omega_N) + 6J(J_{\text{ex}} + \omega_E + \omega_N) \end{array}\right] +$$

$$+n\left(\begin{array}{l} \dfrac{\aleph_{(\text{HFC},\Sigma\text{HF}),\text{intra}}}{90} J(0) + \dfrac{\aleph_{(\text{HFC},\Sigma\text{HF}),\text{intra}}}{120} J(\omega_N) + \dfrac{\aleph_{(\text{HFC},\Sigma\text{HF}),\text{intra}}}{36} J(\omega_E) + \\[2mm] +\dfrac{\aleph_{(\text{HFC},\Delta\text{HF}),\text{intra}}}{720} \left[\begin{array}{l} 3J(J_{\text{ex}} - \omega_E) + 3J(J_{\text{ex}} + \omega_E) + 12J(J_{\text{ex}} - \omega_E - \omega_N) + 12J(J_{\text{ex}} + \omega_E - \omega_N) + \\ +J(J_{\text{ex}} - \omega_E + \omega_N) + 6J(J_{\text{ex}} + \omega_N) + 6J(J_{\text{ex}} + \omega_E + \omega_N) \end{array}\right] \end{array}\right) +$$

$$+\frac{\left[4\aleph_{G,\Delta G} + 2\aleph_{\text{EE},\Delta G}\right]}{240} J(J_{\text{ex}} - \omega_E) + \frac{\left[4\aleph_{G,\Delta G} + 2\aleph_{\text{EE},-\Delta G}\right]}{240} J(J_{\text{ex}} + \omega_E) +$$

$$+\frac{\left[9\Delta_{\text{EE}}^2 + 6\aleph_{G,\Sigma G}\right]}{180} J(\omega_E) + \frac{\Delta_{\text{EE}}^2}{30} J(2\omega_E) \tag{S4}$$

where the symbols are described in the Supplementary Information 5, and we have made a distinction between hyperfine couplings with n protons within the biradical ("intra"), and with one proton that belongs to the solvent ("inter") and could be a target of Overhauser DNP (ODNP). At the fields of interest in our studies, all spectral densities that have the electron and the nuclear Larmor frequency in them can be disregarded. This leaves solely the terms involving zero-frequency spectral densities:

$$R_{1,\text{BRW}} = -R\left[\hat{E}_Z\right] \simeq \frac{\Delta_{\text{EE}}^2}{90} J(0) \tag{S5}$$

and

$$R_{2,\text{BRW}} = -R\left[\hat{E}_+\right] = \frac{\Delta_{\text{EE}}^2}{36} J(0) + \frac{4\aleph_{G,\Sigma G}}{90} J(0) + \frac{\aleph_{(\text{HFC},\Sigma\text{HF}),\text{inter}}}{90} J(0) + n\left(\frac{\aleph_{(\text{HFC},\Sigma\text{HF}),\text{intra}}}{90} J(0)\right) \tag{S6}$$

$R_{1,\text{BRW}}$ is thus dominated by $\Delta_{\text{EE}}^2$, i.e., by the dipolar interaction between electrons; and $R_{2,\text{BRW}}$ is dominated by this term as well as by the second rank scalar products $\aleph_{G,\Sigma G}$ and $\aleph_{\text{HFC},\Sigma\text{HF}}$ between the *g-*

tensor of one electron and the sum of the two $g$-tensors, and by the hyperfine coupling between one electron and one proton, and the sum of the hyperfines of the two electrons and one proton, respectively. The magnitudes of the coefficients in Eq. (S3) and Eq. (S4) for the case of a bistrityl-type biradical, are shown in the Table S2. These coefficients will scale according to spectral densities; Figure S1 show how these BRW-derived $R_1$ and $R_2$ terms change with the biradical's correlation time $\tau_c$. These rates should be compared with the relaxivity contributions arising from the vibrational local modes, which are likely to be in the order of what they were for the monotrityl radical i.e., $\approx 5 \cdot 10^4$ Hz. It follows that for the trityl bis-radical the contribution of these $R_{1,local}$ will no longer be dominant, primarily due to the onset of relaxation effects driven by $\Delta_{EE}^2$ and $\aleph_{G,\Sigma G}$ (the latter mostly at the high fields of interest; Table 1).

**Table S2:** Magnitude of the second-rank norm squared and the scalar products (defined in Supporting Information 5) predicted by Eqs. (S3) and (S6), for a trityl-based biradical with parameters as given in the Table 1.

| $\Delta_A^2$ / $\aleph_{A,B}$ | Magnitude / (rad/s)$^2$ |
|---|---|
| $\Delta_{EE}^2$ | $2 \times 10^{16}$ |
| $\aleph_{G,\Delta G}$ | 472 |
| $\aleph_{G,\Sigma G}$ | $2 \times 10^{17}$ |
| $\aleph_{EE,\Delta G}$ ($\aleph_{EE,-\Delta G}$) | 687699 / -687699 |
| $\aleph_{(HFC,\Sigma HF),intra}$/$\aleph_{(HFC,\Sigma HF),inter}$[1] | $1.30 \times 10^{13}$/$4.9 \times 10^{13}$ |
| $\aleph_{(HFC,\Delta HF),intra}$/$\aleph_{(HFC,\Delta HF),inter}$[1] | $1.34 \times 10^{13}$/$5.1 \times 10^{13}$ |

[1] The intra-molecular dipolar interaction between the electron and the methyl protons in each trityl group of the biradical was computed setting a proton-electron distance equal to 5.3 Å (between the proton and its closest electron; electron/proton hyperfine couplings between the two trityls in the molecule were disregarded). The inter-molecular dipolar interaction between the electron and the solvent was computed setting a proton-electron distance equal to 8.3 Å (again: between the proton and its closest electron only).

Rates do not change also with the increase of the intra-molecular protons n in Eqs. (S3) - (S6), since the term containing $\aleph_{(HFC,\Sigma HF),intra}$ remains much smaller than the term containing $\Delta_{EE}^2$, Fig. S1.
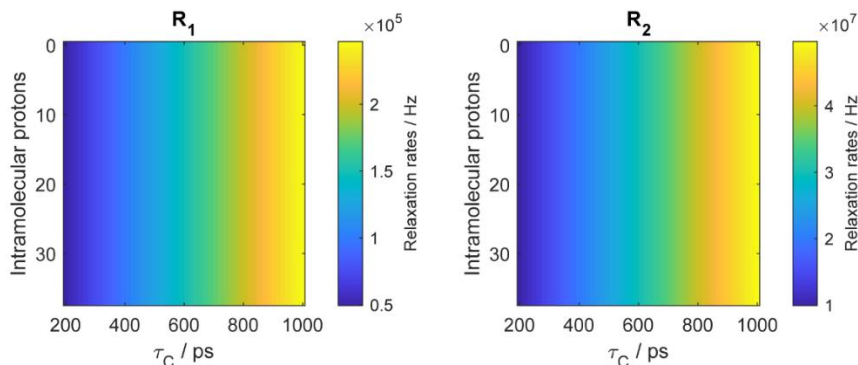


**Fig. S1:** $R_1$ and $R_2$ electron relaxation rates predicted by Eq. (S5) and Eq. (S6) as a function of the $\tau_C$ of the biradical/proton triad and on the number of closest intramolecular protons n to an electron (36 in the case of a model bis-trityl). For these calculations $J_{ex}$ was set equal to $+(\omega_E + \omega_N)$, $B_0$ was set equal to 14.08 T, and other simulation parameters are as given in the Table 1. The absence of a strong dependence with the number of protons reflects the dominant effects of electron-electron dipole and $g$-tensor anisotropies on the relaxation processes, over hyperfine counterparts.

It is enlightening to consider how this model predicts the electron saturation and J-DNP enhancement to proceed, as a function of the available microwave power. Considering that the rotational correlation time of the trityl monomer is about 150 ps –calculated from $\tau_C \simeq r_D^2 / D_t$,[5] where $D_t$ is trityl's translational diffusion constant (in the order of ~$10^{-9}$ m$^2$ s$^{-1}$) and $r_D$ is the minimum distance approach between an electron in the biradical and a proton in the solvent (estimated at about 5-10 Å)– we decided to set the rotational correlation time for the biradical/proton triad equal to $\tau_C \approx 500$ ps (close to what's expected for a trityl biradical). Figure S2 shows the predicted electron saturation and J-DNP

enhancement effects expected for this $\tau_C$ as a function of microwave off-resonance offset and nutation field; similar enhancements and saturation behaviours are predicted for smaller and higher rotational correlation times, up to 1 ns.
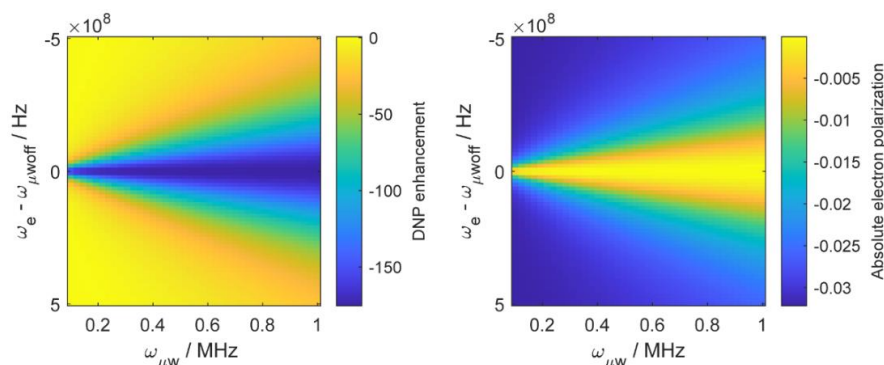


**Fig. S2:** Maximum enhancement (absolute value over the thermal equilibrium) in J-DNP (on the left), achieved between 80-100 ms (depending on the microwave power and $\Delta\omega$), and absolute electron polarization, $\hat{E}_Z$, (on the right), as a function of µw frequency offset from the free electron Larmor frequency and of the µw nutation power, $\omega_{\mu w}$. For these calculations $J_{ex}$ is equal to $\omega_E + \omega_N$, $B_0$ is 14.08 T, $\tau_C$ = 500 ps for the biradical/proton triad, and other simulation parameters as given in the Table 1.

A comparison between the J-DNP and the Overhauser DNP shows that in the electron/nucleus pair system, the ODNP case, the enhancement is strong if $B_o$ < 0.5T, but decays to negligible values if $B_o$ ≥ 3.4 T; this is as expected from classical theories [6-10], while the transient J-DNP is observed also at $B_0$ ≤ 3.4 T.
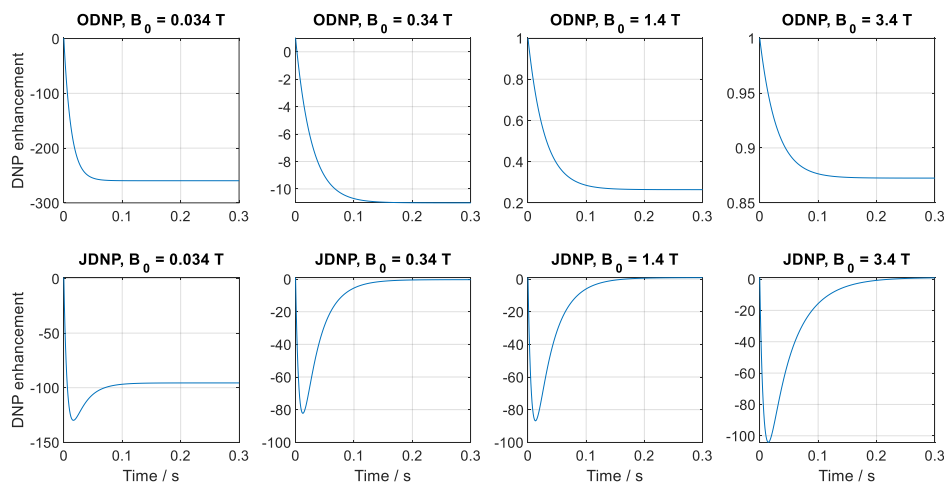


**Fig. S3:** Time domain simulations showing the evolution of the enhancement observed under continuous microwave irradiation of the electrons as a function of $B_0$, in ODNP (on the top) and in JDNP (on the bottom). For ODNP an electron/proton dipolar-coupled pair system with $\tau_c$ = 157 ps (typical of trityl [5]) was assumed; for J-DNP a biradical/proton dipole-coupled triad with $\tau_C$ = 500 ps for the for the biradical/proton triad and $J_{ex}$ = +($\omega_E + \omega_N$) was assumed. Other simulation parameters are given in the Table 1.

Overhauser DNP enhancements higher than those shown in Fig. S3, were observed at the magnetic fields of 1.4 T and 3.4 T, in water doped with trityl based mono radicals.[11,12] Rotational diffusion was the sole DNP-enabling contribution that was considered in our simulations, but translational diffusion can also become an important mechanism of polarization enhancement in actual solvents[11]– explaining the higher enhancements observed in the experimental measurements at these medium magnetic field strengths.

**Supporting Information 2: The Hamiltonian used in the propagation of the biradical/nuclear system – from the Cartesian to the triplet-singlet representations**

The laboratory frame Hamiltonian for a three-spin system composed by two electrons and one proton, where the electrons are connected by dipolar and exchange couplings, and the proton interacts with the electrons through hyperfine (dipolar) coupling only, can be written using single-spin Cartesian operators, as:

$$\hat{H}_{lab.} = \underbrace{\sum_k \hat{\vec{E}}^{(k)} \cdot \mathbf{Z}_E^{(k)} \cdot \vec{B}_0 + \hat{\vec{N}} \cdot \mathbf{Z}_N \cdot \vec{B}_0}_{\text{Zeeman interaction}} + \underbrace{\hat{\vec{E}}^{(1)} \cdot \left( \mathbf{D} + J_{ex} \right) \cdot \hat{\vec{E}}^{(2)}}_{\substack{\text{Dipolar and scalar} \\ \text{inter-electron interaction}}} + \underbrace{\sum_k \hat{\vec{E}}^{(k)} \cdot \mathbf{A}^{(k)} \cdot \hat{\vec{N}}}_{\text{Hyperfine interaction}} \tag{S7}$$

where $\mathbf{Z}_E^{(k)}$ are the Zeeman tensors (including $g$-anisotropy) of electron spins $k=1,2$; $\mathbf{Z}_N$ is the Zeeman tensor of the sole nuclear spin being considered (including the chemical shift anisotropy); $\mathbf{D}$ is the inter-electron dipolar interaction tensor in the point magnetic dipole approximation; $J_{ex}$ is the inter-electron scalar (*aka* "exchange") coupling in angular frequency units; $\mathbf{A}^{(k)}$ is the hyperfine interaction tensors of the nucleus with the indicated electron $k$; $\vec{B}_0$ is the external magnetic field; and $\hat{\vec{E}}^{(1)}$, $\hat{\vec{E}}^{(2)}$ and $\hat{\vec{N}}$ are the Cartesian spin-1/2 operators for the two electrons and nucleus. A rotating frame transformation with respect to the microwave frequency offset using the operator $\omega_{\mu woff} \sum_k \hat{E}_Z^{(k)}$ and preservation of the usual secular and pseudosecular terms, leads to:

$$\hat{H}_{rot.} = \omega_{\Sigma e} \left( \hat{E}_{1Z} + \hat{E}_{2Z} \right) + \omega_{\Delta e} \left( \hat{E}_{1Z} - \hat{E}_{2Z} \right) + \omega_N \hat{N}_Z + \omega_1 \hat{E}_{1Z} \hat{E}_{2Z} + \omega_2 \left( \frac{\hat{E}_{1+} \hat{E}_{2-} + \hat{E}_{1-} \hat{E}_{2+}}{2} \right)$$
$$+ A_\Sigma (\hat{E}_{1Z} + \hat{E}_{2Z}) \hat{N}_Z + A_\Delta (\hat{E}_{1Z} - \hat{E}_{2Z}) \hat{N}_Z + B_\Sigma (\hat{E}_{1Z} + \hat{E}_{2Z}) \hat{N}_X + B_\Delta (\hat{E}_{1Z} - \hat{E}_{2Z}) \hat{N}_X \tag{S8}$$

where $\omega_{\Sigma e}$ and $\omega_{\Delta e}$ are the sum and the difference between the rotating-frame offsets of the two electrons; $A_\Sigma = A_1 + A_2$ and $A_\Delta = A_1 - A_2$; $B_\Sigma = B_1 + B_2$ and $B_\Delta = B_1 - B_2$ are the sum and the difference of the secular and pseudo-secular coefficients describing the hyperfine interaction, respectively; and $\omega_1 = (J_{ex} + 2\mathbf{D})$ and $\omega_2 = (J_{ex} - \mathbf{D})$, where $\mathbf{D}$ is the inter-electron dipolar interaction tensor.

In the $J_{ex} \gg \omega_{\Delta e}$ case, where $\omega_{\Delta e} = \omega_{e1} - \omega_{e2}$ is the difference between the Larmor frequency of the two electrons, the electron Zeeman eigenstates $|\alpha_{e1} \beta_{e2}\rangle$ and $|\beta_{e1} \alpha_{e2}\rangle$ are no longer eigenfunctions of the spin Hamiltonian. We therefore express the Hamiltonian in the singlet/triplet electron basis sets [13,14]:

$$\left. \begin{array}{l} \left| \hat{T}_{+1}^{(e1,e2)} \right\rangle = |\alpha_{e1} \alpha_{e2}\rangle, \; \left| \hat{T}_0^{(e1,e2)} \right\rangle = \frac{1}{\sqrt{2}} \left( |\beta_{e1} \alpha_{e2}\rangle + |\alpha_{e1} \beta_{e2}\rangle \right), \\ \left| \hat{T}_{-1}^{(e1,e2)} \right\rangle = |\beta_{e1} \beta_{e2}\rangle, \; \left| \hat{S}_0^{(e1,e2)} \right\rangle = \frac{1}{\sqrt{2}} \left( |\beta_{e1} \alpha_{e2}\rangle - |\alpha_{e1} \beta_{e2}\rangle \right) \end{array} \right\} \otimes \{\alpha_N, \beta_N\} = \left\{ \begin{array}{l} \left| \hat{S}_0^{(e1,e2)}, \alpha \right\rangle, \; \left| \hat{S}_0^{(e1,e2)}, \beta \right\rangle \\ \left| \hat{T}_0^{(e1,e2)}, \alpha \right\rangle, \; \left| \hat{T}_0^{(e1,e2)}, \beta \right\rangle \\ \left| \hat{T}_{\pm 1}^{(e1,e2)}, \alpha \right\rangle, \; \left| \hat{T}_{\pm 1}^{(e1,e2)}, \beta \right\rangle \end{array} \right\} \tag{S9}$$

where the direct product indicates that the $\{|\alpha_N\rangle, |\beta_N\rangle\}$ Zeeman basis is preserved for the nucleus (proton). The transformation of the three-spin rotating frame Hamiltonian from a Cartesian basis to its singlet/triplet basis can be performed using fictitious spin-½ operators. [15,16] Since the addition of a third nuclear spin has to our knowledge not been reported before, we re-express the rotating-frame Hamiltonian in Eq. (S8), as a sum of terms containing direct products of operators acting in the $\hat{S}_0 \hat{T}_0$ and the $\hat{T}_{+1} \hat{T}_{-1}$ subspaces, with the nuclear Zeeman base. The fictitious spin-1/2 operators that we use in this study to describe the $\hat{S}_0 \hat{T}_0$ and the $\hat{T}_{+1} \hat{T}_{-1}$ subspaces follow from Vega's notation for two-spin fictitious operators[17] and were computed using the SpinDynamica software[18]:

$$\tilde{L}_X^{T_0 S_{0,\alpha}} = \frac{1}{2}\left(\left|\hat{T}_0^{(e1,e2)},\alpha\right\rangle\left\langle\hat{S}_0^{(e1,e2)},\alpha\right| + \left|\hat{S}_0^{(e1,e2)},\alpha\right\rangle\left\langle\hat{T}_0^{(e1,e2)},\alpha\right|\right)$$

$$= \frac{\hat{E}_{1Z}}{4} - \frac{\hat{E}_{2Z}}{4} + \frac{1}{2}\left(\hat{E}_{1Z}\hat{N}_Z\right) - \frac{1}{2}\left(\hat{E}_{2Z}\hat{N}_Z\right) \tag{S10}$$

$$\tilde{L}_X^{T_0 S_{0,\beta}} = \frac{1}{2}\left(\left|\hat{T}_0^{(e1,e2)},\beta\right\rangle\left\langle\hat{S}_0^{(e1,e2)},\beta\right| + \left|\hat{S}_0^{(e1,e2)},\beta\right\rangle\left\langle\hat{T}_0^{(e1,e2)},\beta\right|\right)$$

$$= \frac{\hat{E}_{1Z}}{4} - \frac{\hat{E}_{2Z}}{4} - \frac{1}{2}\left(\hat{E}_{1Z}\hat{N}_Z\right) + \frac{1}{2}\left(\hat{E}_{2Z}\hat{N}_Z\right) \tag{S11}$$

which we combine to obtain:

$$\omega_{\Delta e}\left(\hat{E}_{1Z} - \hat{E}_{2Z}\right) = 2\omega_{\Delta e}\left(\tilde{L}_X^{T_0 S_{0,\alpha}} + \tilde{L}_X^{T_0 S_{0,\beta}}\right) \tag{S12}$$

$$A_{\Delta}\left(\hat{E}_{1Z}N_Z - \hat{E}_{2Z}N_Z\right) = A_{\Delta}\left(\tilde{L}_X^{T_0 S_{0,\alpha}} - \tilde{L}_X^{T_0 S_{0,\beta}}\right) \tag{S13}$$

The longitudinal fictitious ½-spin operators for the electron in the $\hat{S}_0\hat{T}_0$ are:

$$\tilde{L}_Z^{T_0 S_{0,\alpha}} = \frac{1}{2}\left(\left|\hat{T}_0^{(e1,e2)},\alpha\right\rangle\left\langle\hat{T}_0^{(e1,e2)},\alpha\right| - \left|\hat{S}_0^{(e1,e2)},\alpha\right\rangle\left\langle\hat{S}_0^{(e1,e2)},\alpha\right|\right)$$

$$= -\frac{1}{2}\hat{E}_{1X}\hat{E}_{2X} - \frac{1}{2}\hat{E}_{1Y}\hat{E}_{2Y} - \hat{E}_{1X}\hat{E}_{2X}\hat{N}_Z - \hat{E}_{1Y}\hat{E}_{2Y}\hat{N}_Z \tag{S14}$$

$$\tilde{L}_Z^{T_0 S_{0,\beta}} = \frac{1}{2}\left(\left|\hat{T}_0^{(e1,e2)},\beta\right\rangle\left\langle\hat{T}_0^{(e1,e2)},\beta\right| - \left|\hat{S}_0^{(e1,e2)},\beta\right\rangle\left\langle\hat{S}_0^{(e1,e2)},\beta\right|\right)$$

$$= -\frac{1}{2}\hat{E}_{1X}\hat{E}_{2X} - \frac{1}{2}\hat{E}_{1Y}\hat{E}_{2Y} + \hat{E}_{1X}\hat{E}_{2X}\hat{N}_Z + \hat{E}_{1Y}\hat{E}_{2Y}\hat{N}_Z \tag{S15}$$

$$\hat{E}^{T_0 S_{0,\alpha}} = \left(\left|\hat{T}_0^{(e1,e2)},\alpha\right\rangle\left\langle\hat{T}_0^{(e1,e2)},\alpha\right| + \left|\hat{S}_0^{(e1,e2)},\alpha\right\rangle\left\langle\hat{S}_0^{(e1,e2)},\alpha\right|\right)$$

$$= -\hat{E}_{1Z}\hat{E}_{2Z} - 2\hat{E}_{1Z}\hat{E}_{2Z}\hat{N}_Z + \frac{1}{2}\hat{N}_Z + \frac{\mathbf{E}}{4} \tag{S16}$$

$$\hat{E}^{T_0 S_{0,\beta}} = \left(\left|\hat{T}_0^{(e1,e2)},\beta\right\rangle\left\langle\hat{T}_0^{(e1,e2)},\beta\right| + \left|\hat{S}_0^{(e1,e2)},\beta\right\rangle\left\langle\hat{S}_0^{(e1,e2)},\beta\right|\right)$$

$$= -\hat{E}_{1Z}\hat{E}_{2Z} + 2\hat{E}_{1Z}\hat{E}_{2Z}\hat{N}_Z - \frac{1}{2}\hat{N}_Z + \frac{\mathbf{E}}{4} \tag{S17}$$

from which we obtain:

$$\omega_2\left(\tilde{L}_Z^{T_0 S_{0,\alpha}} + \tilde{L}_Z^{T_0 S_{0,\beta}}\right) = \omega_2\left(\hat{E}_{1X}\hat{E}_{2X} + \hat{E}_{1Y}\hat{E}_{2Y}\right) \tag{S18}$$

$$\omega_1\left(\frac{\hat{E}^{T_0 S_{0,\alpha}} + \hat{E}^{T_0 S_{0,\beta}}}{4}\right) = \omega_1\left(-\frac{1}{2}\hat{E}_{1Z}\hat{E}_{2Z} + \frac{\mathbf{E}}{8}\right) \tag{S19}$$

The transverse fictitious ½-spin operators for the proton in the $\hat{S}_0\hat{T}_0$ subspace are:

$$\hat{L}_X^{S_0 T_{0,\alpha\beta}} = \frac{1}{2}\left(\left|\hat{S}_0^{(e1,e2)},\alpha\right\rangle\left\langle\hat{T}_0^{(e1,e2)},\beta\right| + \left|\hat{T}_0^{(e1,e2)},\beta\right\rangle\left\langle\hat{S}_0^{(e1,e2)},\alpha\right|\right)$$

$$= \frac{1}{2}\hat{E}_{1Z}\hat{N}_X - \frac{1}{2}\hat{E}_{2Z}\hat{N}_X + \hat{E}_{1X}\hat{E}_{2Y}\hat{N}_Y - \hat{E}_{1Y}\hat{E}_{2X}\hat{N}_Y \tag{S20}$$

7

$$\tilde{L}_{\mathrm{X}}^{T_0 S_0, \alpha\beta} = \frac{1}{2}\left(\left|\hat{T}_0^{(e1,e2)}, \alpha\right\rangle\left\langle\hat{S}_0^{(e1,e2)}, \beta\right| + \left|\hat{S}_0^{(e1,e2)}, \beta\right\rangle\left\langle\hat{T}_0^{(e1,e2)}, \alpha\right|\right)$$

$$= \frac{1}{2}\hat{E}_{1Z}\hat{N}_{\mathrm{X}} - \frac{1}{2}\hat{E}_{2Z}\hat{N}_{\mathrm{X}} - \hat{E}_{1X}\hat{E}_{2Y}\hat{N}_{\mathrm{Y}} + \hat{E}_{1Y}\hat{E}_{2X}\hat{N}_{\mathrm{Y}} \tag{S21}$$

from which we obtain the pseudo-secular component:

$$B_\Delta\left(\hat{L}_{\mathrm{X}}^{S_0 T_0, \alpha\beta} + \hat{L}_{\mathrm{X}}^{T_0 S_0, \alpha\beta}\right) = B_\Delta\left(\hat{E}_{1Z} - \hat{E}_{2Z}\right)\hat{N}_{\mathrm{X}} \tag{S22}$$

Longitudinal fictitious ½-spin operators for the electron in the $\hat{T}_{+1}\hat{T}_{-1}$ subspace are:

$$\tilde{L}_{\mathrm{Z}}^{T_+ T_{-1}, \alpha} = \frac{1}{2}\left(\left|\hat{T}_{+1}^{(e1,e2)}, \alpha\right\rangle\left\langle\hat{T}_{+1}^{(e1,e2)}, \alpha\right| - \left|\hat{T}_{-1}^{(e1,e2)}, \alpha\right\rangle\left\langle\hat{T}_{-1}^{(e1,e2)}, \alpha\right|\right)$$

$$= \frac{\hat{E}_{1Z}}{4} + \frac{\hat{E}_{2Z}}{4} + \frac{1}{2}\left(\hat{E}_{1Z}\hat{N}_{\mathrm{Z}}\right) + \frac{1}{2}\left(\hat{E}_{2Z}\hat{N}_{\mathrm{Z}}\right) \tag{S23}$$

$$\tilde{L}_{\mathrm{Z}}^{T_+ T_{-1}, \beta} = \frac{1}{2}\left(\left|\hat{T}_{+1}^{(e1,e2)}, \beta\right\rangle\left\langle\hat{T}_{+1}^{(e1,e2)}, \beta\right| - \left|\hat{T}_{-1}^{(e1,e2)}, \beta\right\rangle\left\langle\hat{T}_{-1}^{(e1,e2)}, \beta\right|\right)$$

$$= \frac{\hat{E}_{1Z}}{4} + \frac{\hat{E}_{2Z}}{4} - \frac{1}{2}\left(\hat{E}_{1Z}\hat{N}_{\mathrm{Z}}\right) - \frac{1}{2}\left(\hat{E}_{2Z}\hat{N}_{\mathrm{Z}}\right) \tag{S24}$$

$$\hat{E}^{T_+ T_{-1}, \alpha} = \left(\left|\hat{T}_{+1}^{(e1,e2)}, \alpha\right\rangle\left\langle\hat{T}_{+1}^{(e1,e2)}, \alpha\right| + \left|\hat{T}_{-1}^{(e1,e2)}, \alpha\right\rangle\left\langle\hat{T}_{-1}^{(e1,e2)}, \alpha\right|\right)$$

$$= \hat{E}_{1Z}\hat{E}_{2Z} + 2\hat{E}_{1Z}\hat{E}_{2Z}\hat{N}_{\mathrm{Z}} + \frac{\hat{N}_{\mathrm{Z}}}{2} + \frac{\mathbf{E}}{4} \tag{S25}$$

$$\hat{E}^{T_+ T_{-1}, \beta} = \left(\left|\hat{T}_{+1}^{(e1,e2)}, \beta\right\rangle\left\langle\hat{T}_{+1}^{(e1,e2)}, \beta\right| + \left|\hat{T}_{-1}^{(e1,e2)}, \beta\right\rangle\left\langle\hat{T}_{-1}^{(e1,e2)}, \beta\right|\right)$$

$$= \hat{E}_{1Z}\hat{E}_{2Z} - 2\hat{E}_{1Z}\hat{E}_{2Z}\hat{N}_{\mathrm{Z}} - \frac{\hat{N}_{\mathrm{Z}}}{2} + \frac{\mathbf{E}}{4} \tag{S26}$$

from which we obtain:

$$\omega_{\Sigma e}\left(\hat{E}_{1Z} + \hat{E}_{2Z}\right) = 2\omega_{\Sigma e}\left(\tilde{L}_{\mathrm{Z}}^{T_+ T_{-1}, \alpha} + \tilde{L}_{\mathrm{Z}}^{T_+ T_{-1}, \beta}\right) \tag{S27}$$

$$A_\Sigma\left(\hat{E}_{1Z}\hat{N}_{\mathrm{Z}} + \hat{E}_{2Z}\hat{N}_{\mathrm{Z}}\right) = A_\Sigma\left(\tilde{L}_{\mathrm{Z}}^{T_+ T_{-1}, \alpha} - \tilde{L}_{\mathrm{Z}}^{T_+ T_{-1}, \beta}\right) \tag{S28}$$

$$\omega_1\left(\frac{1}{2}\hat{E}_{1Z}\hat{E}_{2Z} + \frac{\mathbf{E}}{8}\right) = \omega_1\left(\frac{\hat{E}^{T_+ T_{-1}, \alpha} + \hat{E}^{T_+ T_{-1}, \beta}}{4}\right) \tag{S29}$$

Finally, we introduce new transverse fictitious ½-spin operators for the proton in the $\hat{T}_{+1}\hat{T}_{-1}$ subspace given by:

$$\tilde{L}_{\mathrm{X}}^{T_{+1}, \alpha\beta} = \frac{1}{2}\left(\left|\hat{T}_{+1}^{(e1,e2)}, \alpha\right\rangle\left\langle\hat{T}_{+1}^{(e1,e2)}, \beta\right| + \left|\hat{T}_{+1}^{(e1,e2)}, \beta\right\rangle\left\langle\hat{T}_{+1}^{(e1,e2)}, \alpha\right|\right)$$

$$= \frac{1}{2}\hat{E}_{1Z}\hat{N}_{\mathrm{X}} + \frac{1}{2}\hat{E}_{2Z}\hat{N}_{\mathrm{X}} + \hat{E}_{1Z}\hat{E}_{2Z}\hat{N}_{\mathrm{X}} + \frac{\hat{N}_{\mathrm{X}}}{4} \tag{S30}$$

8

$$\hat{L}_X^{T_{-1},\alpha\beta} = \frac{1}{2}\left(\left|\hat{T}_{-1}^{(e1,e2)},\alpha\right\rangle\left\langle\hat{T}_{-1}^{(e1,e2)},\beta\right| + \left|\hat{T}_{-1}^{(e1,e2)},\beta\right\rangle\left\langle\hat{T}_{-1}^{(e1,e2)},\alpha\right|\right)$$

$$= -\frac{1}{2}\hat{E}_{1Z}\hat{N}_X - \frac{1}{2}\hat{E}_{2Z}\hat{N}_X + \hat{E}_{1Z}\hat{E}_{2Z}\hat{N}_X + \frac{\hat{N}_X}{4} \tag{S31}$$

which are needed to describe the pseudo-secular component:

$$B_\Sigma\left(\hat{L}_X^{T_{+1},\alpha\beta} - \hat{L}_X^{T_{-1},\alpha\beta}\right) = B_\Sigma\left(\hat{E}_{1Z} + \hat{E}_{2Z}\right)\hat{N}_X \tag{S32}$$

The sum of these various terms, enables us to rewrite the Hamiltonian in Eq. (S8) under the action of microwave irradiation, as:

$$\hat{H}_{rot} = \hat{H}^{S_0T_0} + \hat{H}^{T_{+1}T_{-1}} + \hat{H}_{\mu w} \tag{S33}$$

where the term acting in the $\hat{S}_0\hat{T}_0$ space is

$$\hat{H}^{S_0T_0} = 2\omega_{\Delta e}\left(\hat{L}_X^{T_0S_0,\alpha} + \hat{L}_X^{T_0S_0,\beta}\right) + A_\Delta\left(\hat{L}_X^{T_0S_0,\alpha} - \hat{L}_X^{T_0S_0,\beta}\right) + B_\Delta\left(\hat{L}_X^{S_0T_0,\alpha\beta} + \hat{L}_X^{T_0S_0,\alpha\beta}\right) +$$

$$- \omega_2\left(\hat{L}_Z^{T_0S_0,\alpha} + \hat{L}_Z^{T_0S_0,\beta}\right) - \omega_1\left(\frac{\hat{E}^{T_0S_0,\alpha} + \hat{E}^{T_0S_0,\beta}}{4}\right) \tag{S34}$$

the term acting in the $\hat{T}_{+1}\hat{T}_{-1}$ space is:

$$\hat{H}^{T_{+1}T_{-1}} = 2\omega_e\left(\hat{L}_Z^{T_{\pm1},\alpha} + \hat{L}_Z^{T_{\pm1},\beta}\right)\hat{R}_y^{T_{\pm1}}(\theta) + \omega_N\hat{N}_Z + B_\Sigma\left(\hat{L}_X^{T_{+1},\alpha\beta} - \hat{L}_X^{T_{-1},\alpha\beta}\right)$$

$$+ A_\Sigma\left(\hat{L}_Z^{T_+T_{-1},\alpha} - \hat{L}_Z^{T_+T_{-1},\beta}\right) + \omega_1\left(\frac{\hat{E}^{T_+T_{-1},\alpha} + \hat{E}^{T_+T_{-1},\beta}}{4}\right) \tag{S35}$$

and $\hat{H}_{\mu w} = \omega_{\mu w}\left(\hat{E}_{1X} + \hat{E}_{2X}\right)$ is the microwave irradiation operator, with $\omega_{\mu w}$ the strength of its nutation frequency. Here $\omega_{\Sigma e}$ and $\omega_{\Delta e} \sim 0$ are the sum and difference of the electron Larmor frequencies in the rotating frame, $\hat{R}_y^{T_{\pm1}}(\theta)$ in Eq. (S35) is a rotation matrix about the y-axis that acts on both the α and β space; its associated $2\omega_e\left(\hat{L}_Z^{T_{\pm1},\alpha} + \hat{L}_Z^{T_{\pm1},\beta}\right)\hat{R}_y^{T_{\pm1}}(\theta)$ term then corresponds to $\omega_e\cos(\theta)\left(\hat{L}_Z^{T_{\pm1},\alpha} + \hat{L}_Z^{T_{\pm1},\beta}\right) + \omega_e\sin(\theta)\left(\hat{E}_{1X} + \hat{E}_{2X}\right)$, with $\theta = \arctan\left(\omega_{\mu w}/\omega_{\Sigma e}\right)$ the angle felt by the electron's effective field, and $\omega_e = \sqrt{\omega_{\Sigma e}^2 + \omega_{\mu w}^2}$ the effective field's strength. The matrix representation of Eq. (S33) is:

| | $\|\hat{S}_0^{(e1,e2)},\alpha\rangle$ | $\|\hat{T}_{+1}^{(e1,e2)},\alpha\rangle$ | $\|\hat{T}_0^{(e1,e2)},\alpha\rangle$ | $\|\hat{T}_{-1}^{(e1,e2)},\alpha\rangle$ | $\|\hat{S}_0^{(e1,e2)},\beta\rangle$ | $\|\hat{T}_{+1}^{(e1,e2)},\beta\rangle$ | $\|\hat{T}_0^{(e1,e2)},\beta\rangle$ | $\|\hat{T}_{-1}^{(e1,e2)},\beta\rangle$ |
|---|---|---|---|---|---|---|---|---|
| $\langle\hat{S}_0^{(e1,e2)},\alpha\|$ | $-\frac{\omega_1}{4}-\frac{\omega_2}{2}+\frac{\omega_N}{2}$ | $0$ | $\frac{A_\Delta}{2}+\omega_{\Delta e}$ | $0$ | $0$ | $0$ | $\frac{B_\Delta}{2}$ | $0$ |
| $\langle\hat{T}_{+1}^{(e1,e2)},\alpha\|$ | $0$ | $\frac{A_\Sigma}{2}+\frac{\omega_1}{4}+\omega_e\cos(\theta)+\frac{\omega_N}{2}$ | $\frac{\omega_e\sin(\theta)}{\sqrt2}$ | $0$ | $0$ | $\frac{B_\Sigma}{2}$ | $0$ | $0$ |
| $\langle\hat{T}_0^{(e1,e2)},\alpha\|$ | $\frac{A_\Delta}{2}+\omega_{\Delta e}$ | $\frac{\omega_e\sin(\theta)}{\sqrt2}$ | $-\frac{\omega_1}{4}+\frac{\omega_1}{2}+\frac{\omega_N}{2}$ | $\frac{\omega_e\sin(\theta)}{\sqrt2}$ | $\frac{B_\Delta}{2}$ | $0$ | $0$ | $0$ |
| $\langle\hat{T}_{-1}^{(e1,e2)},\alpha\|$ | $0$ | $0$ | $\frac{\omega_e\sin(\theta)}{\sqrt2}$ | $-\frac{A_\Sigma}{2}+\frac{\omega_1}{4}-\omega_e\cos(\theta)+\frac{\omega_N}{2}$ | $0$ | $0$ | $0$ | $-\frac{B_\Sigma}{2}$ |
| $\langle\hat{S}_0^{(e1,e2)},\beta\|$ | $0$ | $0$ | $\frac{B_\Delta}{2}$ | $0$ | $-\frac{\omega_1}{4}-\frac{\omega_2}{2}-\frac{\omega_N}{2}$ | $0$ | $-\frac{A_\Delta}{2}+\omega_{\Delta e}$ | $0$ |
| $\langle\hat{T}_{+1}^{(e1,e2)},\beta\|$ | $0$ | $\frac{B_\Sigma}{2}$ | $0$ | $0$ | $0$ | $-\frac{A_\Sigma}{2}+\frac{\omega_1}{4}+\omega_e\cos(\theta)-\frac{\omega_N}{2}$ | $\frac{\omega_e\sin(\theta)}{\sqrt2}$ | $0$ |
| $\langle\hat{T}_0^{(e1,e2)},\beta\|$ | $\frac{B_\Delta}{2}$ | $0$ | $0$ | $-\frac{A_\Delta}{2}+\omega_{\Delta e}$ | $\frac{\omega_e\sin(\theta)}{\sqrt2}$ | $\frac{\omega_e\sin(\theta)}{\sqrt2}$ | $-\frac{\omega_1}{4}+\frac{\omega_2}{2}-\frac{\omega_N}{2}$ | $\frac{\omega_e\sin(\theta)}{\sqrt2}$ |
| $\langle\hat{T}_{-1}^{(e1,e2)},\beta\|$ | $0$ | $0$ | $0$ | $-\frac{B_\Sigma}{2}$ | $0$ | $0$ | $\frac{\omega_e\sin(\theta)}{\sqrt2}$ | $\frac{A_\Sigma}{2}+\frac{\omega_1}{4}-\omega_e\cos(\theta)-\frac{\omega_N}{2}$ |

$$(S36)$$

Notice that these microwave-related terms act solely within the triplet manifold mixing the $\hat{T}_{\pm1}^{(e1,e2)}$ and $\hat{T}_0^{(e1,e2)}$ states, but do not involve the $\hat{S}_0^{(e1,e2)}$ singlet. The latter, however, is not isolated: it gets

connected to $\hat{T}_0^{(e1e2)}$ via the difference in secular hyperfine couplings with the nucleus $A_\Delta$. Additional simulations –not shown– demonstrate that the pseudosecular terms are not essential for describing the J-DNP effect.

**Supporting Information 3: Defining the biradical/nuclear system population operators describing the J-DNP enhancement**

The main text defines $\hat{S}_0\hat{N}_Z$, $\hat{T}_{\pm 1}\hat{N}_Z$ and $\hat{T}_0\hat{N}_Z$ operators and relates these to the differences between the population operators $O_\alpha$ and $O_\beta$ (defined below), leading to the predicted nuclear polarization enhancement. As these three-spin states have to our knowledge not been previously defined, we summarize them here. To do this we rely again on Vega's two-spin triplet/singlet (TS) population operators, [15] and we direct-product them with a nuclear spin state that can be in either the α or β state. These can be written in terms of single-spin product operators, as:

$$
\hat{S}_{0,\alpha} = \left| \hat{S}_0^{(e1,e2)}, \alpha \right\rangle \left\langle \hat{S}_0^{(e1,e2)}, \alpha \right| = \frac{\mathbf{E}}{8} + \frac{\hat{N}_Z}{4} - \frac{1}{4}\left( \hat{E}_{1-}\hat{E}_{2+} \right) - \frac{1}{4}\left( \hat{E}_{1+}\hat{E}_{2-} \right) +
$$
$$
- \frac{1}{2}\left( \hat{E}_{1Z}\hat{E}_{2Z} \right) - \frac{1}{2}\left( \hat{E}_{1-}\hat{E}_{2+}\hat{N}_Z \right) - \frac{1}{2}\left( \hat{E}_{1+}\hat{E}_{2-}\hat{N}_Z \right) - \hat{E}_{1Z}\hat{E}_{2Z}\hat{N}_Z
$$
(S37)

$$
\hat{T}_{\pm 1,\alpha} = \left| \hat{T}_{\pm 1}^{(e1,e2)}, \alpha \right\rangle \left\langle \hat{T}_{\pm 1}^{(e1,e2)}, \alpha \right| = \frac{\mathbf{E}}{8} + \frac{\hat{N}_Z}{4} + \frac{\hat{E}_{1Z}}{4} \pm \frac{\hat{E}_{2Z}}{4} +
$$
$$
+ \frac{1}{2}\left( \hat{E}_{1Z}\hat{E}_{2Z} \right) \pm \frac{1}{2}\left( \hat{E}_{1Z}\hat{N}_Z \right) \pm \frac{1}{2}\left( \hat{E}_{2Z}\hat{N}_Z \right) + \hat{E}_{1Z}\hat{E}_{2Z}\hat{N}_Z
$$
(S38)

$$
\hat{T}_{0,\alpha} = \left| \hat{T}_0^{(e1,e2)}, \alpha \right\rangle \left\langle \hat{T}_0^{(e1,e2)}, \alpha \right| = \frac{\mathbf{E}}{8} + \frac{\hat{N}_Z}{4} + \frac{1}{4}\left( \hat{E}_{1-}\hat{E}_{2+} \right) + \frac{1}{4}\left( \hat{E}_{1+}\hat{E}_{2-} \right) +
$$
$$
- \frac{1}{2}\left( \hat{E}_{1Z}\hat{E}_{2Z} \right) + \frac{1}{2}\left( \hat{E}_{1-}\hat{E}_{2+}\hat{N}_Z \right) + \frac{1}{2}\left( \hat{E}_{1+}\hat{E}_{2-}\hat{N}_Z \right) - \hat{E}_{1Z}\hat{E}_{2Z}\hat{N}_Z
$$
(S39)

$$
\hat{S}_{0,\beta} = \left| \hat{S}_0^{(e1,e2)}, \beta \right\rangle \left\langle \hat{S}_0^{(e1,e2)}, \beta \right| = \frac{\mathbf{E}}{8} - \frac{\hat{N}_Z}{4} - \frac{1}{4}\left( \hat{E}_{1-}\hat{E}_{2+} \right) - \frac{1}{4}\left( \hat{E}_{1+}\hat{E}_{2-} \right) -
$$
$$
+ \frac{1}{2}\left( \hat{E}_{1Z}\hat{E}_{2Z} \right) + \frac{1}{2}\left( \hat{E}_{1-}\hat{E}_{2+}\hat{N}_Z \right) + \frac{1}{2}\left( \hat{E}_{1+}\hat{E}_{2-}\hat{N}_Z \right) + \hat{E}_{1Z}\hat{E}_{2Z}\hat{N}_Z
$$
(S40)

$$
\hat{T}_{\pm 1,\beta} = \left| \hat{T}_{\pm 1}^{(e1,e2)}, \beta \right\rangle \left\langle \hat{T}_{\pm 1}^{(e1,e2)}, \beta \right| = \frac{\mathbf{E}}{8} - \frac{\hat{N}_Z}{4} \pm \frac{\hat{E}_{1Z}}{4} \pm \frac{\hat{E}_{2Z}}{4} +
$$
$$
+ \frac{1}{2}\left( \hat{E}_{1Z}\hat{E}_{2Z} \right) \mp \frac{1}{2}\left( \hat{E}_{1Z}\hat{N}_Z \right) \mp \frac{1}{2}\left( \hat{E}_{2Z}\hat{N}_Z \right) - \hat{E}_{1Z}\hat{E}_{2Z}\hat{N}_Z
$$
(S41)

$$
\hat{T}_{0,\beta} = \left| \hat{T}_0^{(e1,e2)}, \beta \right\rangle \left\langle \hat{T}_0^{(e1,e2)}, \beta \right| = \frac{\mathbf{E}}{8} - \frac{\hat{N}_Z}{4} + \frac{1}{4}\left( \hat{E}_{1-}\hat{E}_{2+} \right) + \frac{1}{4}\left( \hat{E}_{1+}\hat{E}_{2-} \right) -
$$
$$
+ \frac{1}{2}\left( \hat{E}_{1Z}\hat{E}_{2Z} \right) - \frac{1}{2}\left( \hat{E}_{1-}\hat{E}_{2+}\hat{N}_Z \right) - \frac{1}{2}\left( \hat{E}_{1+}\hat{E}_{2-}\hat{N}_Z \right) + \hat{E}_{1Z}\hat{E}_{2Z}\hat{N}_Z
$$
(S42)

Taking suitable differences among these states, leads to the longitudinal fictitious operators used in the main text (Figures 4-5) to describe how singlet and triplet states enhance the nuclear polarization:

$$
\hat{S}_0^{(e1,e2)}\hat{N}_Z = \frac{1}{2}\left( \left| \hat{S}_0^{(e1,e2)}, \alpha \right\rangle \left\langle \hat{S}_0^{(e1,e2)}, \alpha \right| - \left| \hat{S}_0^{(e1,e2)}, \beta \right\rangle \left\langle \hat{S}_0^{(e1,e2)}, \beta \right| \right)
$$
$$
= \frac{\hat{N}_Z}{4} - \frac{1}{2}\left( \hat{E}_{1-}\hat{E}_{2+}\hat{N}_Z + \hat{E}_{1+}\hat{E}_{2-}\hat{N}_Z \right) - \hat{E}_{1Z}\hat{E}_{2Z}\hat{N}_Z
$$
(S43)

$$\hat{T}_{\pm 1}^{(e1,e2)}\hat{N}_{\mathrm{Z}} = \frac{1}{2}\left(\left|\hat{T}_{\pm 1}^{(e1,e2)},\alpha\right\rangle\left\langle\hat{T}_{\pm 1}^{(e1,e2)},\alpha\right| - \left|\hat{T}_{\pm 1}^{(e1,e2)},\beta\right\rangle\left\langle\hat{T}_{\pm 1}^{(e1,e2)},\beta\right|\right)$$

$$= \frac{\hat{N}_{\mathrm{Z}}}{4} \pm \frac{1}{2}\left(\hat{E}_{1\mathrm{Z}}\hat{N}_{\mathrm{Z}} + \hat{E}_{2\mathrm{Z}}\hat{N}_{\mathrm{Z}}\right) + \hat{E}_{1\mathrm{Z}}\hat{E}_{2\mathrm{Z}}\hat{N}_{\mathrm{Z}}$$

(S44)

$$\hat{T}_{0}^{(e1,e2)}\hat{N}_{\mathrm{Z}} = \frac{1}{2}\left(\left|\hat{T}_{0}^{(e1,e2)},\alpha\right\rangle\left\langle\hat{T}_{0}^{(e1,e2)},\alpha\right| - \left|\hat{T}_{0}^{(e1,e2)},\beta\right\rangle\left\langle\hat{T}_{0}^{(e1,e2)},\beta\right|\right)$$

$$= \frac{\hat{N}_{\mathrm{Z}}}{4} + \frac{1}{2}\left(\hat{E}_{1-}\hat{E}_{2+}\hat{N}_{\mathrm{Z}} + \hat{E}_{1+}\hat{E}_{2-}\hat{N}_{\mathrm{Z}}\right) - \hat{E}_{1\mathrm{Z}}\hat{E}_{2\mathrm{Z}}\hat{N}_{\mathrm{Z}}$$

(S45)

$$\hat{T}_{\pm 1}^{(e1,e2)}\hat{N}_{\mathrm{Z}} = \frac{1}{2}\left(\left|\hat{T}_{\pm 1}^{(e1,e2)},\alpha\right\rangle\left\langle\hat{T}_{\pm 1}^{(e1,e2)},\alpha\right| - \left|\hat{T}_{\pm 1}^{(e1,e2)},\beta\right\rangle\left\langle\hat{T}_{\pm 1}^{(e1,e2)},\beta\right|\right)$$

## Supporting Information 4: Additional Redfield-derived relaxation rates for the biradical/nuclear system

The main text presented a simplified version of the relaxation rates of $\hat{S}_{0,\alpha/\beta}$, $\hat{T}_{0,\alpha/\beta}$ and $\hat{T}_{\pm 1,\alpha,\beta}$, whose full expressions are provided here. For $\hat{S}_{0,\alpha/\beta}$ these were:

$$-R\left[\hat{S}_{0,\beta}\right] = \frac{\Delta_{\text{AHF}}^2}{180} J\left(J_{\text{ex}} - \omega_{\text{E}} + \omega_{\text{N}}\right) + \frac{\Delta_{\text{AHF}}^2}{30} J\left(J_{\text{ex}} + \omega_{\text{E}} + \omega_{\text{N}}\right) + \frac{\Delta_{\text{CSA}}^2}{15} J\left(\omega_{\text{N}}\right) + \frac{\Delta_{\text{AHF}}^2}{60} J\left(J_{\text{ex}} + \omega_{\text{N}}\right) +$$
$$+ \frac{\left[\Delta_{\text{AHF}}^2 + 4\aleph_{\Delta\text{G},\Delta\text{G-AHF}}\right]}{90} J\left(J_{\text{ex}}\right) + \frac{\left[\Delta_{\text{AHF}}^2 + 4\aleph_{\Delta\text{G},\Delta\text{G-AHF}}\right]}{120} J\left(J_{\text{ex}} - \omega_{\text{E}}\right) + \frac{\left[\Delta_{\text{AHF}}^2 + 4\aleph_{\Delta\text{G},\Delta\text{G-AHF}}\right]}{120} J\left(J_{\text{ex}} + \omega_{\text{E}}\right) \tag{S46}$$

and

$$-R\left[\hat{S}_{0,\alpha}\right] = \frac{\Delta_{\text{AHF}}^2}{180} J\left(J_{\text{ex}} + \omega_{\text{E}} - \omega_{\text{N}}\right) + \frac{\Delta_{\text{AHF}}^2}{30} J\left(J_{\text{ex}} - \omega_{\text{E}} - \omega_{\text{N}}\right) + \frac{\Delta_{\text{CSA}}^2}{15} J\left(\omega_{\text{N}}\right) + \frac{\Delta_{\text{AHF}}^2}{60} J\left(J_{\text{ex}} - \omega_{\text{N}}\right) +$$
$$+ \frac{\left[\Delta_{\text{AHF}}^2 + 4\aleph_{\Delta\text{G},\Delta\text{G+AHF}}\right]}{90} J\left(J_{\text{ex}}\right) + \frac{\left[\Delta_{\text{AHF}}^2 + 4\aleph_{\Delta\text{G},\Delta\text{G+AHF}}\right]}{120} J\left(J_{\text{ex}} - \omega_{\text{E}}\right) + \frac{\left[\Delta_{\text{AHF}}^2 + 4\aleph_{\Delta\text{G},\Delta\text{G+AHF}}\right]}{120} J\left(J_{\text{ex}} + \omega_{\text{E}}\right) \tag{S47}$$

For the $\hat{T}_{+1,\alpha/\beta}$ states these were:

$$-R\left[\hat{T}_{+1,\beta}\right] = \frac{\Delta_{\text{AHF}}^2}{180} J\left(J_{\text{ex}} + \omega_{\text{E}} - \omega_{\text{N}}\right) + \frac{\left[\Delta_{\text{AHF}}^2 + 4\aleph_{\Delta\text{G},\Delta\text{G-AHF}}\right]}{120} J\left(J_{\text{ex}} + \omega_{\text{E}}\right) +$$
$$+ \frac{\left[\Delta_{\Sigma\text{HF}}^2 + 4\aleph_{\text{CSA,CSA}+\Sigma\text{HF}}\right]}{60} J\left(\omega_{\text{N}}\right) + \frac{\left[5\Delta_{\Sigma\text{HF}}^2 + 12\aleph_{\text{EE}+\Sigma\text{G},(\text{EE}+\Sigma\text{G})-\Sigma\text{HF}}\right]}{360} J\left(\omega_{\text{E}}\right) + \frac{\Delta_{\text{EE}}^2}{15} J\left(2\omega_{\text{E}}\right) \tag{S48}$$

and

$$-R\left[\hat{T}_{+1,\alpha}\right] = \frac{\Delta_{\text{AHF}}^2}{30} J\left(J_{\text{ex}} + \omega_{\text{E}} + \omega_{\text{N}}\right) + \frac{\left[\Delta_{\text{AHF}}^2 + 4\aleph_{\Delta\text{G},\Delta\text{G+AHF}}\right]}{120} J\left(J_{\text{ex}} + \omega_{\text{E}}\right) +$$
$$+ \frac{\left[\Delta_{\Sigma\text{HF}}^2 + 4\aleph_{\text{CSA,CSA}+\Sigma\text{HF}}\right]}{60} J\left(\omega_{\text{N}}\right) + \frac{\left[5\Delta_{\Sigma\text{HF}}^2 + 4\aleph_{\text{EE}+\Sigma\text{G},(\text{EE}+\Sigma\text{G})+\Sigma\text{HF}}\right]}{120} J\left(\omega_{\text{E}}\right) + \frac{\Delta_{\text{EE}}^2}{15} J\left(2\omega_{\text{E}}\right) \tag{S49}$$

For the $\hat{T}_{0,\alpha/\beta}$, the self-relaxation rates are

$$-R\left[\hat{T}_{0,\beta}\right] = \frac{\Delta_{\text{CSA}}^2}{15} J\left(\omega_{\text{N}}\right) + \frac{\Delta_{\text{AHF}}^2}{60} J\left(J_{\text{ex}} - \omega_{\text{N}}\right) +$$
$$+ \frac{\left[\Delta_{\text{AHF}}^2 + 4\aleph_{\Delta\text{G},\Delta\text{G}-\text{AHF}}\right]}{90} J\left(J_{\text{ex}}\right) + \frac{\left[6\Delta_{\text{EE}}^2 + 5\Delta_{\Sigma\text{HF}}^2 + 6\aleph_{\Sigma\text{G},\Sigma\text{G}-\Sigma\text{HF}}\right]}{90} J\left(\omega_{\text{E}}\right) \tag{S50}$$

and

$$-R\left[\hat{T}_{0,\alpha}\right] = \frac{\Delta_{\text{CSA}}^2}{15} J\left(\omega_{\text{N}}\right) + \frac{\Delta_{\text{AHF}}^2}{60} J\left(J_{\text{ex}} + \omega_{\text{N}}\right) +$$
$$+ \frac{\left[\Delta_{\text{AHF}}^2 + 4\aleph_{\Delta\text{G},\Delta\text{G}+\text{AHF}}\right]}{90} J\left(J_{\text{ex}}\right) + \frac{\left[6\Delta_{\text{EE}}^2 + 5\Delta_{\Sigma\text{HF}}^2 + 6\aleph_{\Sigma\text{G},\Sigma\text{G}+\Sigma\text{HF}}\right]}{90} J\left(\omega_{\text{E}}\right) \tag{S51}$$

And for $\hat{T}_{-1,\alpha/\beta}$ the self-relaxation rates were:

$$-R\left[\hat{T}_{-1,\beta}\right] = \frac{\Delta_{\text{AHF}}^2}{30} J\left(J_{\text{ex}} - \omega_{\text{E}} - \omega_{\text{N}}\right) + \frac{\left[\Delta_{\text{AHF}}^2 + 4\aleph_{\Delta\text{G},\Delta\text{G}-\text{AHF}}\right]}{120} J\left(J_{\text{ex}} - \omega_{\text{E}}\right) +$$
$$+ \frac{\left[\Delta_{\Sigma\text{HF}}^2 + 4\aleph_{\text{CSA,CSA}-\Sigma\text{HF}}\right]}{60} J\left(\omega_{\text{N}}\right) + \frac{\left[5\Delta_{\Sigma\text{HF}}^2 + 4\aleph_{\text{EE}-\Sigma\text{G,EE}-\Sigma\text{G}+\Sigma\text{HF}}\right]}{120} J\left(\omega_{\text{E}}\right) + \frac{\Delta_{\text{EE}}^2}{15} J\left(2\omega_{\text{E}}\right) \tag{S52}$$

and

$$-R\left[\hat{T}_{-1,\alpha}\right] = \frac{\Delta^2_{\Delta HF}}{180} J\left(J_{ex} - \omega_E + \omega_N\right) + \frac{\left[\Delta^2_{\Delta HF} + 4\aleph_{\Delta G,\Delta G+\Delta HF}\right]}{120} J\left(J_{ex} - \omega_E\right) +$$

$$+ \frac{\left[\Delta^2_{\Sigma HF} + 4\aleph_{CSA,CSA-\Sigma HF}\right]}{60} J\left(\omega_N\right) + \frac{\left[5\Delta^2_{\Sigma HF} + 12\aleph_{EE-\Sigma G,EE-\Sigma G-\Sigma HF}\right]}{360} J\left(\omega_E\right) + \frac{\Delta^2_{EE}}{15} J\left(2\omega_E\right)$$

(S53)

These expressions were all derived taking the possibility of having the spins' relaxation driven by the nuclear chemical shift anisotropy tensor (**CSA**), by $\Delta \mathbf{G} = \mathbf{G_1} - \mathbf{G_2}$ and by $\Delta \mathbf{HF} = \mathbf{HFC_1} - \mathbf{HFC_2}$ anisotropies deriving from tensors associated to the differences between the two *g*- and electron/nuclear hyperfine coupling tensors, respectively; by tensors $\Sigma \mathbf{G} = \mathbf{G_1} + \mathbf{G_2}$ and $\Sigma \mathbf{HF} = \mathbf{HFC_1} + \mathbf{HFC_2}$ associated to the sums of these two electron *g*- and hyperfine tensors, and by the **EE** interaction representing the dipolar tensor between the two. As is usual in spin relaxation theory [19,20], all these rates contain combinations of second-rank norms squared $\Delta^2_A$ of all the aforementioned tensors **A**, second-rank scalar products $\aleph_{A,B}$ of 3x3 tensors **A** and **B** [3], and linear combinations of these products among various tensors, as given in Supporting Information 5. Figures S4 and S5 below expand this matter further, by showing how rates of $\hat{S}_{0,\alpha/\beta}$, $\hat{T}_{0,\alpha/\beta}$ and $\hat{T}_{\pm 1,\alpha/\beta}$ vary, when $J_{ex}$ matches $\pm(\omega_E + \omega_N)$ − this time as a function of $B_0$ and $\tau_C$.
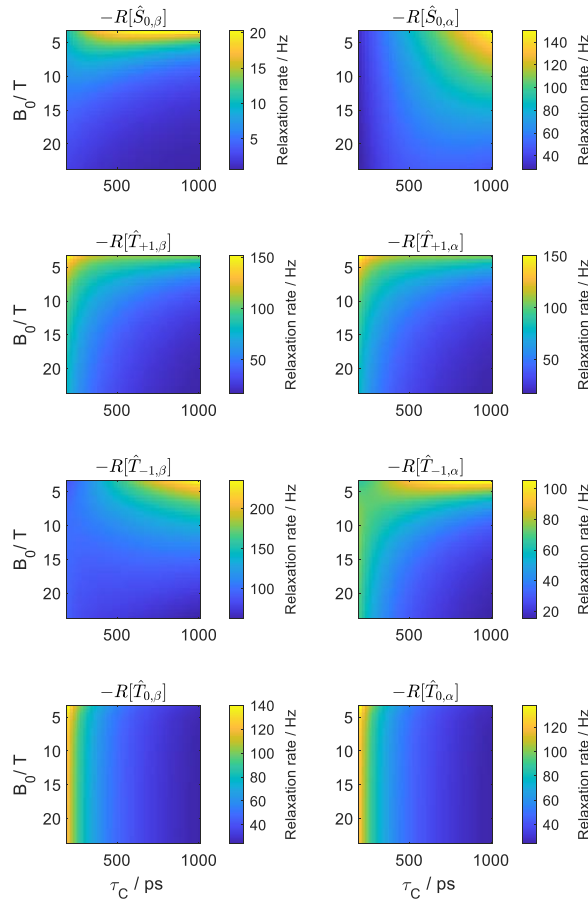


**Fig. S4:** Numerically calculated self-relaxation rates of $\hat{S}_{0,\alpha/\beta}$, $\hat{T}_{0,\alpha/\beta}$ and $\hat{T}_{\pm 1,\alpha/\beta}$ as a function of $B_0$ and of the $\tau_C$ of the biradical/proton triad, when $J_{ex}$ is positive and equal to $J_{ex} = -(\omega_E + \omega_N)$. Other simulation parameters are given in Table 1.
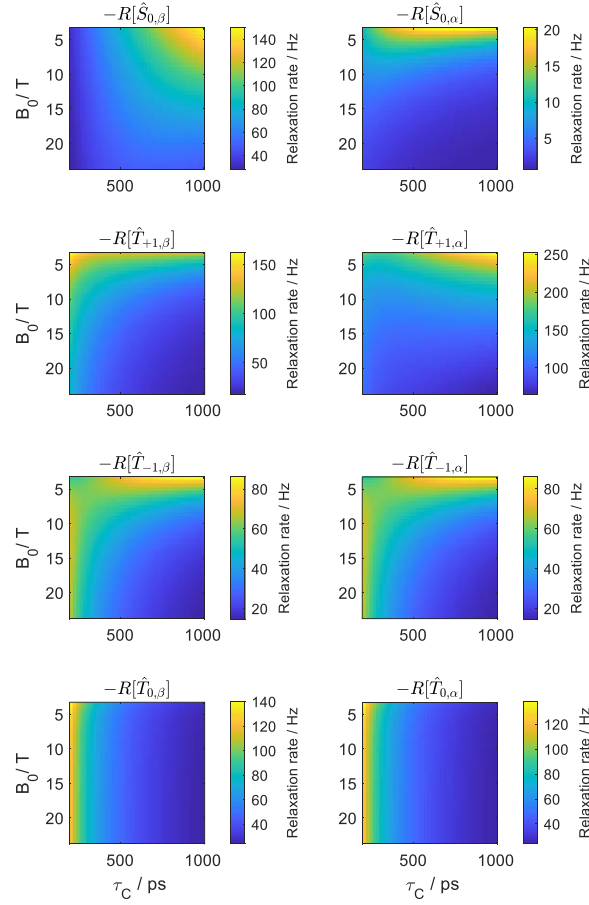
**Fig. S5:** Numerically calculated self-relaxation rates of $\hat{S}_{0,\alpha/\beta}$, $\hat{T}_{0,\alpha/\beta}$ and $\hat{T}_{\pm1,\alpha/\beta}$ as a function of $B_0$ and of the $\tau_C$ of the biradical/proton triad, when $J_{ex}$ is negative and equal to $J_{ex} = +(\omega_E + \omega_N)$. Other simulation parameters are given in Table 1.

Notice how these rates decrease with magnetic field and change differentially for $\alpha/\beta$ states with the correlation time. The main text presented how the rates of $\hat{S}_{0,\alpha/\beta}$, $\hat{T}_{0,\alpha/\beta}$ and $\hat{T}_{\pm1,\alpha/\beta}$ changed with exchange coupling and magnetic field, according to numerical and analytical predictions. For completion this section derives the expressions predicted by this theory, for the $\hat{N}_Z\hat{T}_{\pm1}$, $\hat{N}_Z\hat{T}_0$ and $\hat{S}_0\hat{N}_Z$ states.

$$-R\left[\hat{N}_Z\hat{S}_0\right] = \frac{2\Delta_{CSA}^2}{15}J(\omega_N) + \frac{\Delta_{\Delta HF}^2}{120}\left[J(J_{ex}-\omega_N) + J(J_{ex}+\omega_N)\right] +$$
$$+ \frac{\Delta_{\Delta HF}^2}{60}\left[J(J_{ex}-\omega_E-\omega_N) + J(J_{ex}+\omega_E+\omega_N)\right] +$$
$$+ \frac{\Delta_{\Delta HF}^2}{360}\left[J(J_{ex}+\omega_E-\omega_N) + J(J_{ex}-\omega_E+\omega_N)\right] +$$
$$+ \frac{\Delta_{\Delta HF}^2 + 4\Delta_{\Delta G}^2}{90}J(J_{ex}) + \frac{\Delta_{\Delta HF}^2 + 4\Delta_{\Delta G}^2}{120}\left[J(J_{ex}-\omega_E) + J(J_{ex}+\omega_E)\right]$$

(S54)

$$-R\left[\hat{N}_Z\hat{T}_{+1}\right] = \frac{\Delta_{EE}^2}{15}J(2\omega_E) + \frac{\Delta_{\Delta HF}^2}{360}J(J_{ex}+\omega_E-\omega_N) + \frac{\Delta_{\Delta HF}^2}{60}J(J_{ex}+\omega_E+\omega_N) +$$
$$\frac{\Delta_{\Delta HF}^2 + 4\Delta_{\Delta G}^2}{120}J(J_{ex}+\omega_E) + \frac{\left[\Delta_{\Sigma HF}^2 + 4\aleph_{CSA,CSA+\Sigma HF}^2\right]}{30}J(\omega_N) + \frac{\left[5\Delta_{\Sigma HF}^2 + 6\Delta_{EE+\Sigma G}^2\right]}{180}J(\omega_E)$$

(S55)

15

$$-R\left[\hat{N}_{\mathrm{Z}}\hat{T}_{-1}\right]=\frac{\Delta_{\mathrm{EE}}^{2}}{15}J\left(2\omega_{\mathrm{E}}\right)+\frac{\Delta_{\Delta\mathrm{HF}}^{2}}{360}J\left(J_{\mathrm{ex}}-\omega_{\mathrm{E}}+\omega_{\mathrm{N}}\right)+\frac{\Delta_{\Delta\mathrm{HF}}^{2}}{60}J\left(J_{\mathrm{ex}}-\omega_{\mathrm{E}}-\omega_{\mathrm{N}}\right)+$$

$$\frac{\Delta_{\Delta\mathrm{HF}}^{2}+4\Delta_{\Delta\mathrm{G}}^{2}}{120}J\left(J_{\mathrm{ex}}-\omega_{\mathrm{E}}\right)+\frac{\left[\Delta_{\Sigma\mathrm{HF}}^{2}+4\aleph_{\mathrm{CSA,CSA-\Sigma HF}}\right]}{30}J\left(\omega_{\mathrm{N}}\right)+\frac{\left[5\Delta_{\Sigma\mathrm{HF}}^{2}+6\Delta_{\mathrm{EE-\Sigma G}}^{2}\right]}{180}J\left(\omega_{\mathrm{E}}\right)$$

(S56)

$$-R\left[\hat{N}_{\mathrm{Z}}\hat{T}_{0}\right]=\frac{2\Delta_{\mathrm{CSA}}^{2}}{15}J\left(\omega_{\mathrm{N}}\right)+\frac{\Delta_{\Delta\mathrm{HF}}^{2}}{120}\left[J\left(J_{\mathrm{ex}}-\omega_{\mathrm{N}}\right)+J\left(J_{\mathrm{ex}}+\omega_{\mathrm{N}}\right)\right]+$$

$$+\frac{\Delta_{\Delta\mathrm{HF}}^{2}+4\Delta_{\Delta\mathrm{G}}^{2}}{90}J\left(J_{\mathrm{ex}}\right)+\frac{\left[6\Delta_{\mathrm{EE}}^{2}+5\Delta_{\Sigma\mathrm{HF}}^{2}+6\Delta_{\Sigma\mathrm{G}}^{2}\right]}{90}J\left(\omega_{\mathrm{E}}\right)$$

(S57)

where the meaning of the various constants and functions are the same as in Eqs. (S46) - (S53). Figures S6 and S7 present how these rates depend on the magnetic fields and on the rotational correlation times.
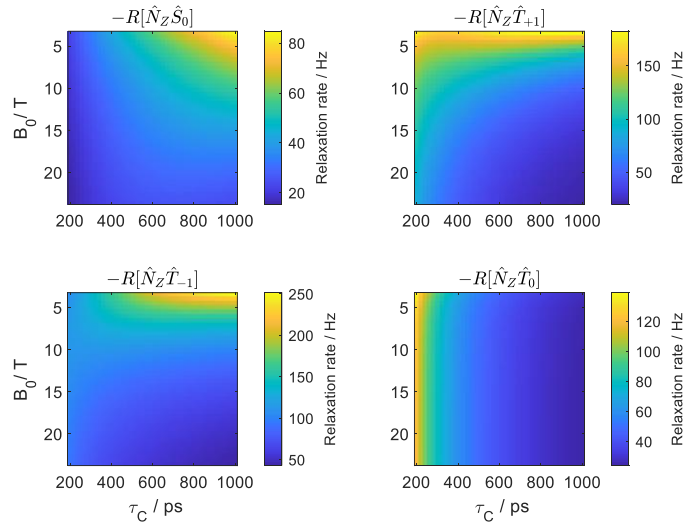


**Fig. S6:** Self-relaxation rates of $\hat{N}_{\mathrm{Z}}\hat{S}_{0}$, $\hat{N}_{\mathrm{Z}}\hat{T}_{\pm 1}$ and $\hat{N}_{\mathrm{Z}}\hat{T}_{0}$ states calculated as a function of $B_{0}$ and of the $\tau_{\mathrm{C}}$ of the biradical/proton triad, for $J_{\mathrm{ex}}=-(\omega_{\mathrm{E}}+\omega_{\mathrm{N}})$. Other simulation parameters are given in Table 1.
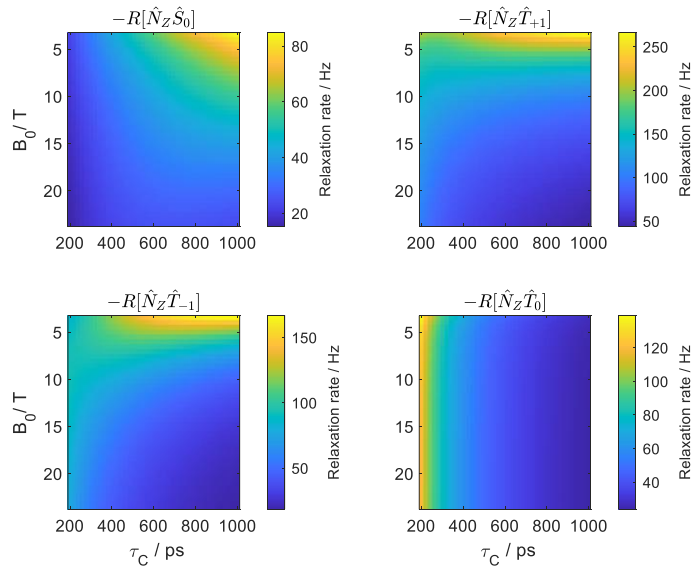


**Fig. S7:** Self-relaxation rates of $\hat{N}_{\mathrm{Z}}\hat{S}_{0}$, $\hat{N}_{\mathrm{Z}}\hat{T}_{\pm 1}$ and $\hat{N}_{\mathrm{Z}}\hat{T}_{0}$ states calculated as a function of $B_{0}$ and of the $\tau_{\mathrm{C}}$ of the biradical/proton triad, at $J_{\mathrm{ex}}=+(\omega_{\mathrm{E}}+\omega_{\mathrm{N}})$. Other simulation parameters are given in Table 1.

**Supporting Information 5: Additional information about the Redfield analysis of the biradical/nuclear system**

The rate expressions derived by the Redfield theory analysis for the three-spin system in Eqs. (5)-(12) of the main text, and in Eqs. S1 - S6 and S46 -S57 in the Supporting Information, were expressed on the basis of the second-rank square norms and scalar products of 3x3 tensors:

$$\aleph_{\mathbf{A,B}} = \frac{\Delta^2_{\mathbf{A+B}} - \Delta^2_{\mathbf{A-B}}}{4}$$

$$\Delta^2_{\mathbf{A}} = a^2_{XX} + a^2_{YY} + a^2_{ZZ} - a_{XX}a_{YY} - a_{XX}a_{ZZ} - a_{YY}a_{ZZ} +$$

$$+ \frac{3}{4}\left[ \left(a_{XY} + a_{YX}\right)^2 + \left(a_{XZ} + a_{ZX}\right)^2 + \left(a_{YZ} + a_{ZY}\right)^2 \right] \tag{S58}$$

where $\Delta_{\mathbf{A}}$ is the second-rank norm squared of a tensor **A** and $\aleph_{\mathbf{A,B}}$ is the second-rank scalar product between two 3×3 interaction tensors **A** and **B**. They can also contain linear combinations of more than two tensors and are often expressed based on the following algebraic relation:

$$\Delta^2_{\mathbf{A-B}} = \Delta^2_{\mathbf{A}} + \Delta^2_{\mathbf{B}} - 2\aleph_{\mathbf{A,B}}, \; \Delta^2_{\mathbf{A+B}} = \Delta^2_{\mathbf{A}} + \Delta^2_{\mathbf{B}} + 2\aleph_{\mathbf{A,B}},$$

$$\Delta^2_{\mathbf{A+(B+C)}} = \Delta^2_{\mathbf{A}} + \Delta^2_{\mathbf{B+C}} + 2\aleph_{\mathbf{A,B+C}}, \; \Delta^2_{\mathbf{A-(B+C)}} = \Delta^2_{\mathbf{A}} + \Delta^2_{\mathbf{B+C}} - 2\aleph_{\mathbf{A,B+C}},$$

$$\Delta^2_{\mathbf{A-B}} = \aleph_{\mathbf{A-B,A-B}}, \Delta^2_{\mathbf{A+B}} = \aleph_{\mathbf{A+B,A+B}},$$

$$\aleph_{\mathbf{A,B+C}} = \aleph_{\mathbf{A,B}} + \aleph_{\mathbf{A,C}}, \; \aleph_{\mathbf{A,B-C}} = \aleph_{\mathbf{A,B}} - \aleph_{\mathbf{A,C}},$$

$$\aleph_{\mathbf{A+(D+E),B+C}} = \aleph_{\mathbf{A,B+C}} + \aleph_{\mathbf{D+E,B+C}},$$

$$\aleph_{\mathbf{A-D,B+C}} = \aleph_{\mathbf{A,B+C}} + \aleph_{\mathbf{-D,B+C}}$$

$$\aleph_{\mathbf{A-B,-(C-D)}} + \aleph_{\mathbf{A-B,A-B}} = \aleph_{\mathbf{A-B,(A-B)-(C-D)}}, \aleph_{\mathbf{A+B,-(C+D)}} + \aleph_{\mathbf{A+B,A+B}} = \aleph_{\mathbf{A+B,(A+B)-(C+D)}}$$

$$\aleph_{\mathbf{A-B,C-D}} + \aleph_{\mathbf{A-B,A-B}} = \aleph_{\mathbf{A-B,(A-B)+(C-D)}}, \aleph_{\mathbf{A+B,C+D}} + \aleph_{\mathbf{A+B,A+B}} = \aleph_{\mathbf{A+B,(A+B)+(C+D)}} \tag{S59}$$

**Supporting Information 6: J-DNP enhancements for other kinds of biradical/nuclear systems**

Table 1 in the main text focused on one combination of electron and nuclear spin coupling parameters, leading to the features noted in the paper. The two electrons had identical *g*-tensors, with electron and nuclear Zeeman couplings made anisotropic for the sake of realism. This section summarized four additional sets of combinations, as per the parameters summarized in Table S3. These include (i) the same coupling parameters as in Table 1 but for a different placement of the nucleus, which was now assumed devoid of chemical shift anisotropy; (ii) same parameters as in Table 1 but now with electron sites endowed with identical rhombic *g*-tensors; (iii) same parameters as in Table 1 but now with the electrons devoid of *g*-anisotropies; (iv) same parameters as in Table 1 but now with electron sites endowed with different isotropic *g*-tensors. The systems in the Table S3 thus contain axial, rhombic and isotropic *g*-tensors –in the latter case with coinciding and non-coinciding isotropic values. For the sake of conciseness, only the time-domain J-DNP transient enhancements were calculated for these scenarios –using the single optimal $J_{ex} = +(\omega_E + \omega_N)$ but as function of $B_o$ and $\tau_c$. These are shown in Figures S8-S11. Note how similar is the behaviour for all these systems, when compared with that shown in Figure 3.

**Table S3:** Biradical / proton magnetic resonance parameters used in the simulations shown in Figures S8-S11. Each electron in the biradical had its parameters modelled on a trityl center, and the nucleus was placed along the linker closer to one of the electrons. $B_o$, $J_{ex}$ and $\tau_c$ for the biradical/proton triad were set as described in the figures; all other hyperfine coupling parameters relied on the distances.

| Parameter | System i | System ii | System iii | System iv |
|---|---|---|---|---|
| [1]H chemical shift tensor, ppm | [10  10  10] | [5  10  20] | [5  10  20] | [5  10  20] |
| *g*-tensor[1] for the electron 1 and 2, Bohr magneton | [2.0032 2.0032 2.0026] | [2.0030 2.0025 2.0020] | [2.0032 2.0032 2.0032] | $g_1$=[2.0032 2.0032 2.0032] $g_2$=[2.0027 2.0027 2.0027] |
| [1]H coordinates, [x y z], Å | [-3 0.5 1.3] | [-3 0.5 1.3] | [-3 0.5 1.3] | [-3 0.5 1.3] |
| Electron 1 coordinates, [x y z], Å | [0  0  -9.37] | [0  0  -9.37] | [0  0  -9.37] | [0  0  -9.37] |
| Electron 2 coordinates, [x y z], Å | [0  0  9.37] | [0  0  9.37] | [0  0  9.37] | [0  0  9.37] |
| Scalar relaxation modulation depth /GHz | 3 | 3 | 3 | 1 |
| Scalar relaxation modulation time, ps | 1 | 1 | 1 | 1 |
| Temperature/ K | 298 | 298 | 298 | 298 |
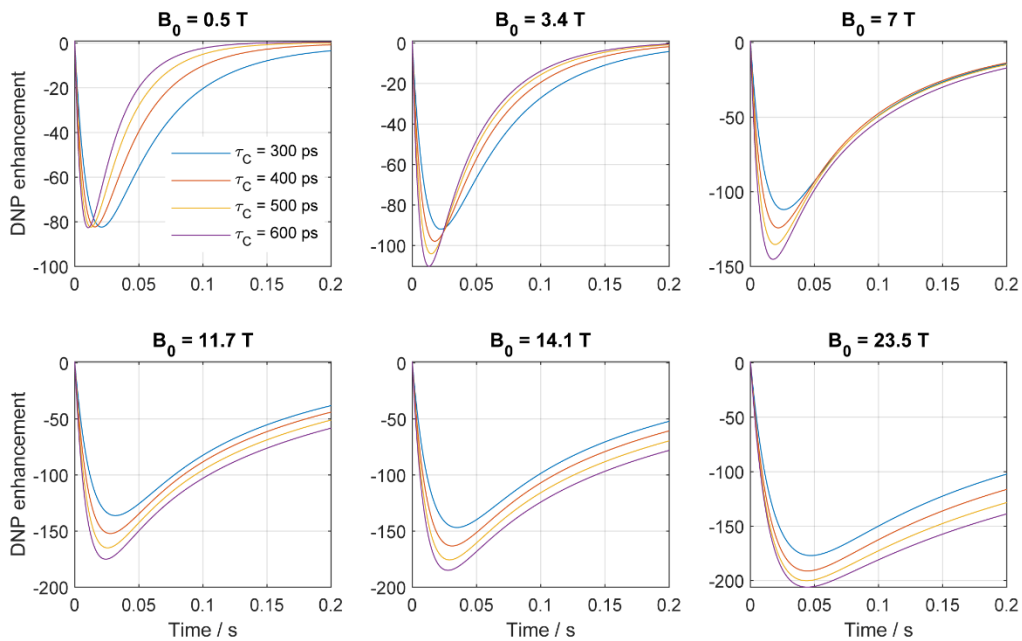
**Fig. S8:** Time domain simulations showing the evolution of the transient J-DNP enhancement as a function of $B_0$ and of $\tau_C$. For all fields $J_{ex}$ was tuned to $+(\omega_E + \omega_N)$, using the parameters of the system (i) in Table S3.
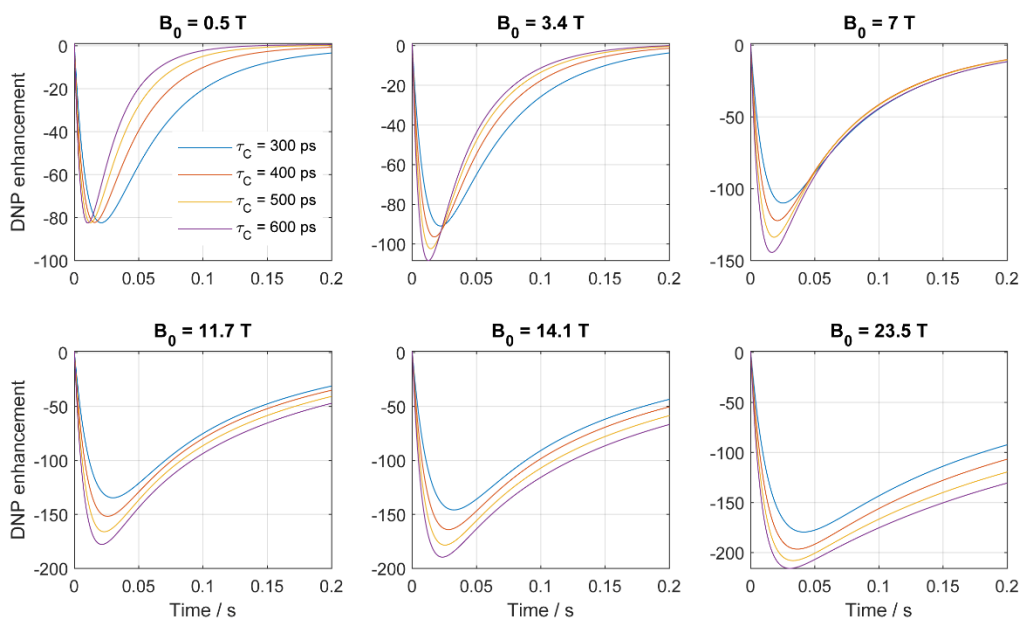


**Fig. S9:** Time domain simulations showing the evolution of the transient J-DNP enhancement as a function of $B_0$ and of $\tau_C$. For all fields $J_{ex}$ was tuned to $+(\omega_E + \omega_N)$ , using the parameters of the system (ii) in Table S3.
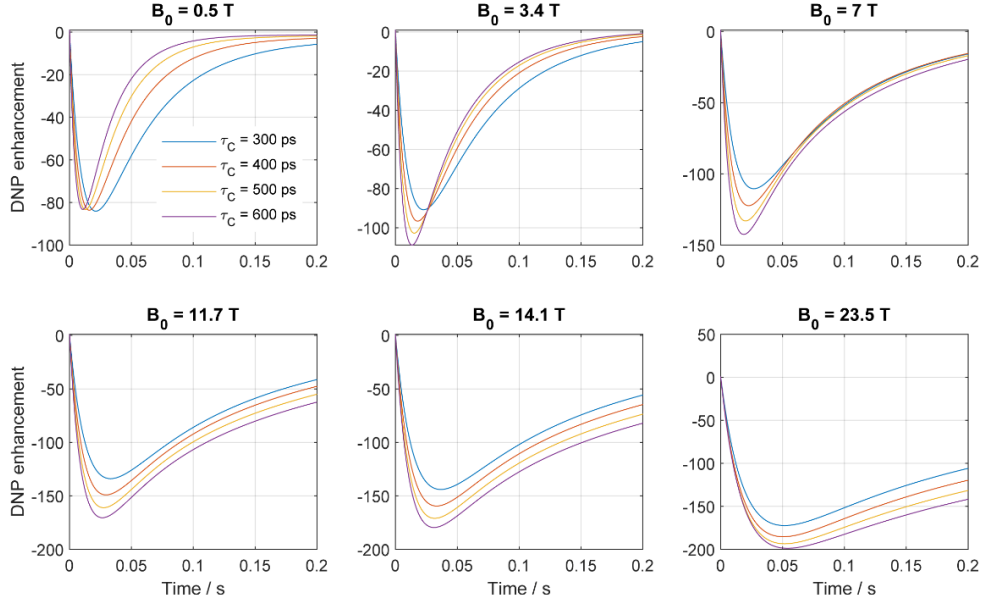
**Fig. S10:** Time domain simulations showing the evolution of the transient J-DNP enhancement as a function of $B_0$ and of $\tau_C$. For all fields $J_{ex}$ was tuned to $+(\omega_E + \omega_N)$, using the parameters of the system (iii) in Table S3.
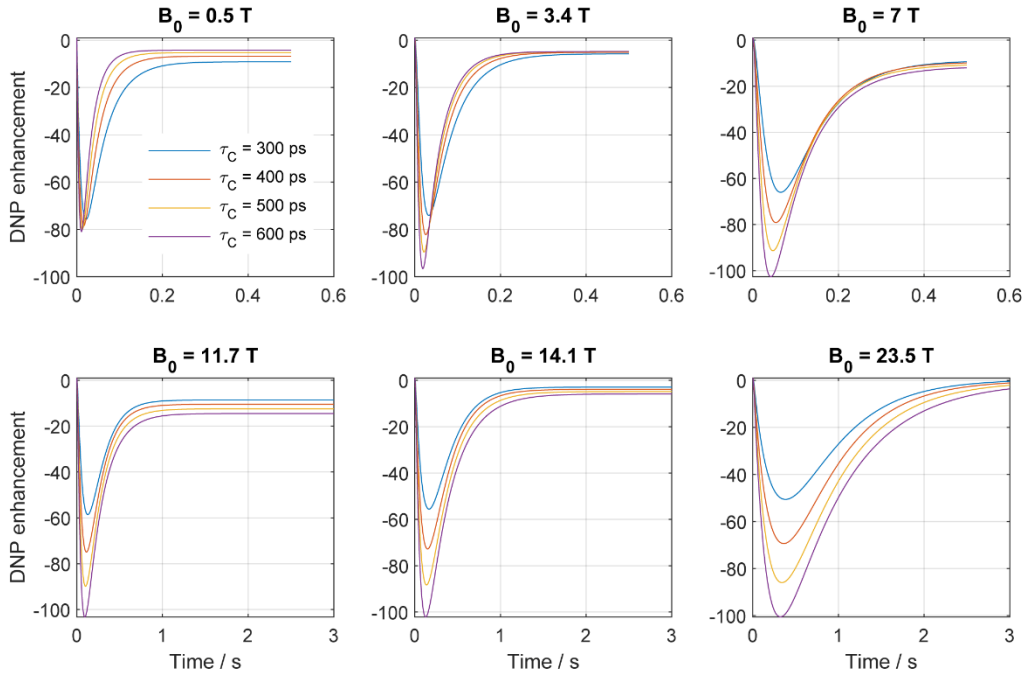


**Fig. S11:** Time domain simulations showing the evolution of the transient J-DNP enhancement as a function of $B_0$ and of $\tau_C$. For all fields $J_{ex}$ was tuned to $+(\omega_E + \omega_N)$, using the parameters of the system (iv) in Table S3.

Despite the noted similarity among all these cases, it is important to remark that cases will also arise where the J-DNP enhancement will be "killed", Figures S12 - S14 include three of such instances. In the first of these, the nucleus is symmetrically placed in-between two identical electrons, that would otherwise lead to enhancement; this makes the differential "CIDNP-like" effect stop working. J-DNP requires differential hyperfine couplings driving a differential relaxation-based "nuclear spin-state filter", in their absence, for instance if the nucleus is symmetrically placed between the two electrons (Supporting Figure S12), no enhancement results. The second case involves two electron sites endowed with different anisotropic *g*-tensors (Supporting Figure S13); in such instance the $\aleph_{\Delta G,\Delta G\pm\Delta HF}$

terms overtake the $\Delta^2_{\text{HFC}}$ in Eqs. (5) − (12), robbing J-DNP for its efficiency even when $J_{\text{ex}} = \pm (\omega_{\text{E}} + \omega_{\text{N}})$. Notice that this does not happen when $g_{1,\text{iso}} = g_{2,\text{iso}}$ (Supporting Figure S11), as the $\aleph_{\Delta\text{G},\Delta\text{G}\pm\Delta\text{HF}}$ terms still remain then smaller than $\Delta^2_{\text{HFC}}$. Finally, the enhancement will tend to zero if the nucleus remains too distant from the biradical: for instance, a proton placed 20 Å away from the bi-radical that may require over 1 s to achieve significant polarization gains, a time by which the DNP effect will lose against competing pathways. Interestingly, despite J-DNP's origin in effects related to second-rank spherical anisotropies, its nuclear enhancement never changes sign (Supporting Figure S14).
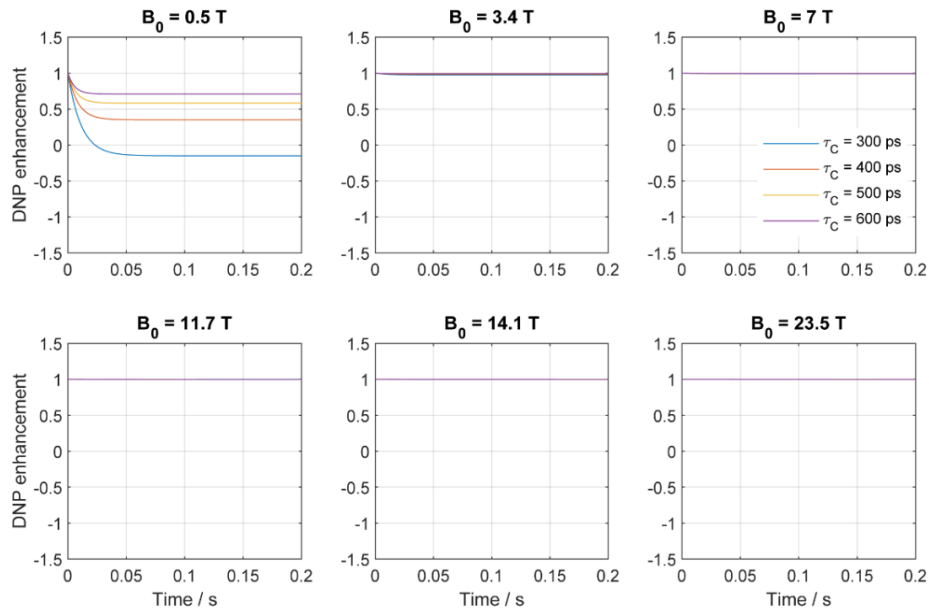


**Fig. S12:** Time domain simulations showing the evolution of the transient J-DNP enhancement as a function of $B_0$ and of $\tau_{\text{C}}$. For all fields $J_{\text{ex}}$ was tuned to $+(\omega_{\text{E}} + \omega_{\text{N}})$, using the parameters of the system in Table 1, but with the proton placed symmetrically in the biradical's centre (i.e, at [0 0 0] Å).
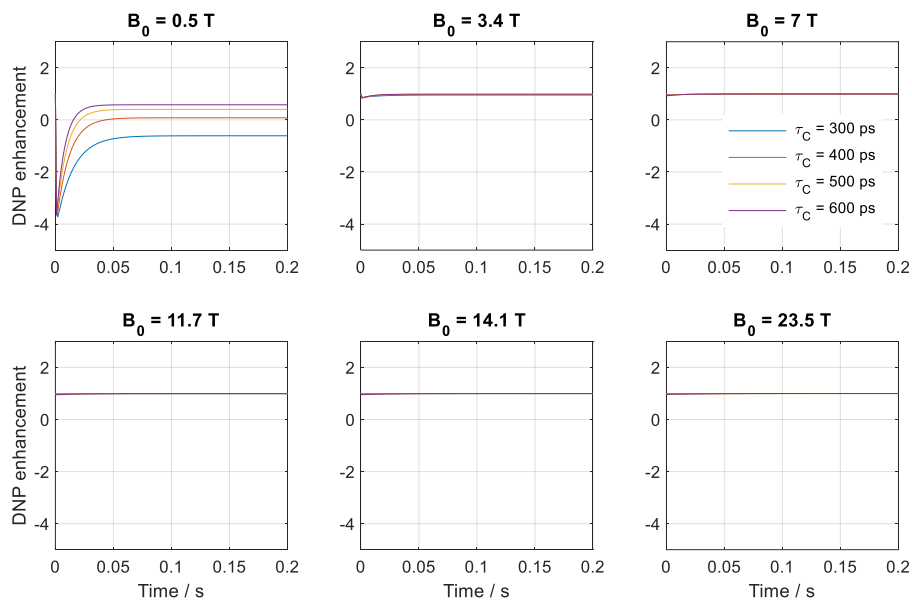


**Fig. S13:** Time domain simulations showing the evolution of the transient J-DNP enhancement as a function of $B_0$ and of $\tau_{\text{C}}$. For all fields $J_{\text{ex}}$ was tuned to $+(\omega_{\text{E}} + \omega_{\text{N}})$, using the same parameters as in Table 1 but now with electron sites endowed with different anisotropic g-tensors equal to: $g_1$=[2.0032 2.0032 2.0026] and $g_2$=[2.0032 2.0032 2.0023].
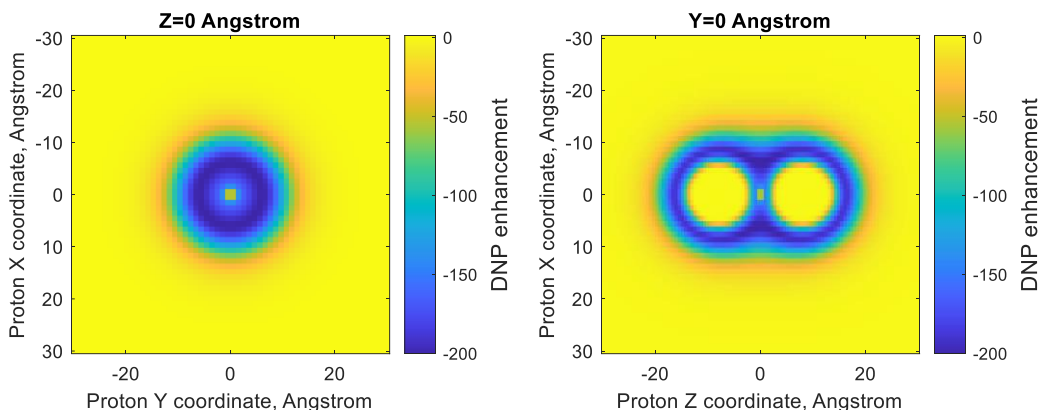
**Fig. S14:** Maximum enhancement (amplitude of $\hat{N}_Z$ normalized to the thermal equilibrium value of a single proton at the same magnetic field) achieved within 20 ms of microwave irradiation at the electron Larmor frequency, as a function of random $^1$H-coordinates surrounding a model biradical. Parameters included $B_0$ = 14.08 T, $\tau_c$ = 500 ps of the biradical/proton triad, other conditions as given in Table 1. Notice the negative enhancement displayed by all positions surrounding the radical. This is important, as otherwise the spatial averaging brought about by molecular translations, could end up being smaller or even zero.

# References

1       Owenius, R., Eaton, G. R. & Eaton, S. S. Frequency (250 MHz to 9.2 GHz) and viscosity dependence of electron spin relaxation of triarylmethyl radicals at room temperature. *J Magn Reson* **172**, 168, (2005).

2       Yong, L. *et al.* Electron spin relaxation of triarylmethyl radicals in fluid solution. *J Magn Reson* **152**, 156, (2001).

3       Blicharski, J. Nuclear magnetic relaxation by anisotropy of the chemical shift. *Z Naturforsch Pt A* **27**, 1456 (1972).

4       Kuprov, I., Wagner-Rundell, N. & Hore, P. Bloch-Redfield-Wangsness theory engine implementation using symbolic processing software. *J Magn Reson* **184**, 196 (2007).

5       Ardenkjaer-Larsen, J. H. *et al.* EPR and DNP properties of certain novel single electron contrast agents intended for oximetric imaging. *J Magn Reson* **133**, 1, (1998).

6       Hausser, K. H. & Stehlik, D. Dynamic nuclear polarization in liquids, in Advances in Magnetic and Optical Resonance. Vol. 3, p.79-139 (Elsevier, 1968).

7       Griesinger, C. *et al.* Dynamic nuclear polarization at high magnetic fields in liquids. *Prog Nucl Magn Reson Spectrosc* **64**, 4, (2012).

8       Prisner, T., Denysenkov, V. & Sezer, D. Liquid state DNP at high magnetic fields: Instrumentation, experimental results and atomistic modelling by molecular dynamics simulations. *J Magn Reson* **264**, 68, (2016).

9       Parigi, G., Ravera, E., Bennati, M. & Luchinat, C. Understanding Overhauser Dynamic Nuclear Polarisation through NMR relaxometry. *Mol Phys* **117**, 888, (2019).

10      Levien, M., Hiller, M., Tkach, I., Bennati, M. & Orlando, T. Nitroxide Derivatives for Dynamic Nuclear Polarization in Liquids: The Role of Rotational Diffusion. *J Phys Chem Lett* **11**, 1629, (2020).

11      Wind, R. A. & Ardenkjaer-Larsen, J. H. 1H DNP at 1.4 T of water doped with a triarylmethyl-based radical. *J Magn Reson* **141**, 347-354, (1999).

12      Hofer, P. *et al.* Field dependent dynamic nuclear polarization with radicals in aqueous solution. *J Am Chem Soc* **130**, 3254, (2008).

13      Hu, K. N., Debelouchina, G. T., Smith, A. A. & Griffin, R. G. Quantum mechanical theory of dynamic nuclear polarization in solid dielectrics. *J Chem Phys* **134**, 125105, (2011).

14      Bajaj, V. S. *et al.* 250 GHz CW gyrotron oscillator for dynamic nuclear polarization in biological solid state NMR. *J Magn Reson* **189**, 251, (2007).

15      Vega, S. Fictitious spin 1/2 operator formalism for multiple quantum NMR. *J Chem Phys* **68**, 5518 (1978).

16      Ernst, R. R., Bodenhausen, G. & Wokaun, A. Principles of Nuclear Magnetic Resonance in One and Two Dimensions.  p.610 (Oxford: Clarendon Press, 1987).

17      Pileio, G. Singlet NMR methodology in two-spin-1/2 systems. *Prog Nucl Magn Reson Spectrosc* **98-99**, 1, (2017).

18      Bengs, C. & Levitt, M. H. SpinDynamica: Symbolic and numerical magnetic resonance in a Mathematica environment. *Magn Reson Chem* **56**, 374, (2018).

19      Redfield, A. *The theory of relaxation processes, in Advances in Magnetic and Optical Resonance*. Vol. 1, p.1-32 (Elsevier, 1965).

20      Goldman, M. Formal theory of spin--lattice relaxation. *J Magn Reson* **149**, 160, (2001).